LBL-10952

Lawrence Berkeley Laboratory
UNIVERSITY OF CALIFORNIA

Materials & Molecular Research Division

MASTER

Al_2O_3 ADHERENCE ON CoCrAl ALLOYS

Lori McConnell Kingsley
(M.S. thesis)

April 1980

Prepared for the U.S. Department of Energy under Contract W-7405-ENG-48

Al_2O_3 ADHERENCE ON CoCrAl ALLOYS

Table of Contents

Al_2O_3 ADHERENCE ON CoCrAl ALLOYS

Lori McConnell Kingsley

Material Science and Mineral Engineering
Lawrence Berkeley Laboratory, University of California
Berkeley, California 94720

ABSTRACT

Adherence of protective oxides on NiCrAl and CoCrAl superalloys has been promoted by a dispersion of a highly oxygen reactive element or its oxide being produced within the protection system. Two aspects of this subject are investigated here: 1) the use of Al_2O_3 as both the dispersion and protective oxide; and 2) the production of an HfO_2 dispersion while simultaneously aluminizing the alloy.

It was found that 1) an Al_2O_3 dispersion will act to promote the adherence of an external scale of Al_2O_3 to a degree comparable to previously tested dispersions and 2) an HfO_2 dispersion comparable to that produced by a "Rhines pack" treatment is produced during aluminization.

To my parents,

for 25 years of love, support, and encouragement

and

To my husband and daughter,

for all the love and joy in my life.

ACKNOWLEDGMENTS

I wish express my gratitude for the encouragement and support shown me by Professor Dave Whittle, for the many conversations that sparked my curiosity and cleared up my confusions, and for his abundance of understanding and good humor concerning my conflicts of personal and professional lives.

Many thanks to Dr. Ibrihim Allam for many enlightening conversations, general "how-to" help, and a real sense of humor. Thanks also to Dr. Haroun Hindam and other members of our research group for sharing their knowledge so willingly.

Thanks to the many people of Building 62 that have helped with me so many things the past two years, especially to Herb Riebe for his patient hours, to Weyland Wong and the High Bay gang for their help, to Don Krieger for getting me started in the first place, to Jim Severns for helping me recover from explosive mistakes.

Special thanks to Lee Johnson and Brian Pope for all their help and conversation, and to Carmen Hubbard for typing the final drafts.

And to my buddies—gratitude and so much more for the long hours of conversation, encouragement, and friendship. Thanks to Sue for all the time and typing. Thanks to Cil for her insight and couch. And thanks to Cil, Pete, and Lenny for all the laughter and companionship that helped so much.

Last, but not least, I want to acknowledge the effort, patience, love, and encouragement poured into my life and education by my parents and especially by my husband, Pat. Without Pat and Carrie my life and achievements would mean so much less to me.

This work was supported by the Division of Materials Science, Office of Basic Research, U. S. Department of Energy, Contract No. 7405-ENG-48.

INTRODUCTION

In the use of gas turbines the greatest efficiency can be obtained using high turbine entry temperatures and high compression ratios. The materials developed to withstand high temperatures and high compression ratios without losing their strength are referred to as "superalloys."

The "superalloys" do, however, have limitations. They are degraded at these high operating temperatures by creep, mechanical fatigue and oxidation. Much work has been done to develop materials for which corrosion and oxidation are controlled to the point where the life of the turbine parts is limited only by creep and fatigue.

Superalloys

The superalloys used in the blades of a turbine are nickel- and cobalt-based. The lighter nickel alloys are most appropriate for the rotor blades, which see somewhat lower temperatures and higher stresses. The use of the lighter material avoids the large centrifugal forces that would result if the rotating blades were made of the heavier cobalt alloys. Nickel or cobalt alloys are used for the stationary vanes of the turbine that operate at higher temperatures (by $\sim 100°C$) and see lower stresses.

The cobalt-based superalloys exhibit a higher surface stability, being more resistant to surface degradation by hot corrosion. Oxidation is the larger problem at high temperatures, however, and the resistance

of these alloys is not as good as that of the nickel-based alloys. A higher chromium content in the cobalt alloys generally leads to a better surface stability in this regard.

The higher temperature strength of the cobalt-based alloys is obtained from complex refractory metal carbides.[1] However, the same additions that give the superalloys their strength lower the materials' resistance to surface degradation by oxidation, hot corrosion, and thermal fatigue. Thus the need for the high strength with oxidation resistance has led to the use of coatings that are applied to the part to be used after its manufacture.

Oxidation Protection Systems

The major protection systems used for superalloys and some of their characteristics are listed in Table I. Coatings can be used to protect the underlying alloy from oxidation while strength is no longer such an important factor as it is with the alloy itself. The protection systems depend upon the ability of the coating to form a slow-growing protective oxide barrier to separate the underlying alloy from the oxidizing environment. In order for an oxide to provide such a barrier it must have the following characteristics:

1) low concentration of ionic defects
2) low vaporization rate
3) high melting point
4) low dissociation pressure
5) high negative free energy of formation (high thermodynamic stability)

Table I. Major protection systems for superalloys.

Class	Typical Methods of Application	Major Elements Applied	Major Protective Constituents	Primary Protective Surface Oxide	Major Physical Characteristics
Aluminide coatings	Pack cementation Slurry + diffusion Electrophoresis + diffusion Hot dipping Chemical vapor deposition Fused salt metalliding Physical vapor deposition	Al,Cr,Si Al,Cr,Si Al,Cr,Si Al Al,Cr,Si Al,Cr,Si Al,Cr,Si Ti,Fe,Co,Y	NiAl on nickel alloys CoAl on cobalt alloys	Al_2O_3 Cr_2O_3 SiO_2 Complex spinels	Hard, brittle at ambient temperature becoming softer and more ductile at high temperature.
Metallic claddings	Isostatic hot-pressure bond Physical vapor deposition Plasma spraying Thermal spray + fusion	Ni,Cr,Al, Fe,Si,B, Co,etc.	NiCr alloys NiCrAl alloys FeCrAl alloys CoCrAl alloys	Al_2O_3 Cr_2O_3 SiO_2 Complex Spinels	Low strength but good ductility over a wide temperature range.
Glass coatings	Slurry + fire Thermal spray Surface reaction	Si,B, Alkali metals, Cr	SiO silicate glass	SiO_2 silicate glass	Hard, brittle at ambient temperature gradually softening at high temperature.

6) freedom from pores, cracks, or other short-circuit paths

7) good adherence to the underlying metal substrate, even under thermal cycling conditions where adherence is more difficult due to differences in thermal expansion in the oxide and alloy.

These characteristics are found to varying degrees in Al_2O_3, Cr_2O_3, and SiO_2. Some of their properties are given in Table II.

Table II

Oxide	$\Delta G°_f$(1000°C)[3] per mole O_2 (kcal)	m.p.[4] °C	ΔH_{dec}[4] (kcal)	log P_{O_2}
Al_2O_3	-204	2030	266.8	-34.7
Cr_2O_3	-125	2400	180	-21.8
SiO_2	-153	1610	210.2	-28.0

SiO_2 may be oxidized to form a gas species[5] at high temperatures, or react with metallic ions to form complex molten oxides. Also, the presence of Si in Co-20Cr alloy has been shown to cause problems with scale adhesion upon cooling as well as during isothermal oxidation treatments.[6] Cr_2O_3 oxidizes above 1000°C to form the volatile CrO_3[7,8] and the rate of volatilization is significant under conditions of high gas velocity.[9]

Al_2O_3, on the other hand, does not form volatile species and has less tendency than Cr_2O_3 to form compound oxides. It has high wear and thermal shock resistance. Due to these factors most major protection systems for superalloys are coatings which form Al_2O_3 or Al_2O_3-rich scales as barrier against rapid oxidation.[5,10,11]

Whether or not Al_2O_3 will form as a protective external scale or as particles of oxide internal to the alloy is dependent on several factors.[12-16]

1) The relative thermodynamic stability of Al_2O_3 must be higher compared to the stability of other oxide phases that may be present.

2) The bulk alloy composition must provide enough Al to be oxidized for continuous scale production and re-supply in case of spalling.

3) The alloy interdiffusion coefficients should be large to enhance precipitation of Al near the surface for external scale formation.

4) Oxygen solubility and diffusivity in the alloy determines internal oxidation possibilities.

5) The relative growth rates of oxides of all components of the alloy will determine development and overgrowth rates and undercutting processes in scale development.

6) Epitaxy and substructural effects, as they affect the defect structure near the alloy surface, can affect the oxide/alloy mismatch or vacancy condensation.

External conditions such as temperature, pressure and methods of heating will of course affect these factors. In view of these factors and the dependence of the steady-state scale structure on the initial nucleation process, it is difficult to apply any exacting theory to the process of oxidation in multicomponent superalloys.

Al_2O_3 Protection of Cobalt Alloys

For cobalt-based coatings with sufficient aluminum to produce a protective Al_2O_3 layer, a CoAl phase is the "reservoir" providing the aluminum. In a cobalt-aluminum system at 1000 °C, 13 w/o Al is needed for protection. Lesser amounts are needed at lower temperatures.[17] Diffusion of aluminum within the substrate, either outward to provide a new supply to replaced spalled scale[18] or inward due to a concentration gradient, may lead to failure. The aluminum-rich β CoAl phase loses aluminum to become αCo, which is easily oxidized to a non-adherent CoO scale.

Beyond 1000°C additions of other elements are required if protection based on an Al_2O_3 layer is to be effective. In protection systems provided by metallic cladding or overlays, the Co-Cr-Al alloys are used. When added to NiAl alloys, chromium is known to lower the concentration of Al required to provide the continuous layer of Al_2O_3 on the surface.[19] CoCrAl systems are similar to these NiCrAl alloys except for a higher oxygen solubility and lower interdiffusion coefficients in the CoCrAl alloys.[20] In this case the use of Cr as an oxygen "getter" becomes even more important to prevent the formation of Al_2O_3 as internal oxide particles with a consequent lack of Al for the external scale production.[21]

It has been proposed that, with the addition of chromium, Cr_2O_3 is formed during the initial stages of oxidation, leading to a reduction in the effective oxygen pressure at the Cr_2O_3/alloy interface and a lower rate of oxygen flux into the alloy. As a consequence, aluminum

is allowed to diffuse to the alloy/scale interface without forming internal oxide particles, and a layer of protective Al_2O_3 can form beneath the thin initial oxide layer.[21,22]

The lowered Al content of the alloy gives it greater ductility and consequently thermal fatigue cracking is not as common in these cladding materials as it is when an aluminide layer is applied directly to the part to be protected.

Figure 1 is an "oxide map" for the CoCrAl systems, developed by Wallwork and Hed.[23] The various alloys have been divided into four groups according to the oxides formed at 1100°C.

Group I: These alloys contain up to 10 w/o chromium and 8 w/o Al. The oxides produced on these alloys consist of an outer dense layer of columnar CoO and an inner porous layer of CoO mixed with Al_2O_3, Cr_2O_3, and $Co(Cr,Al)_2O_4$.

Group II: The alloys in this group contain large concentrations of Al and Cr and form a duplex scale over a discontinuous $Co(CrAl)_2O_4$ spinel in a CoO matrix.

Group III: Chromium content here is high enough so that a continuous external scale of Cr_2O_3 is formed with α-Al_2O_3 precipitating as internal oxide particles.

Group IV: Enough Al is present in these alloys to form α-Al_2O_3 as a continuous external scale.

Scale/Alloy Adherence

For any scale to be protective there are two major requirements:[24]

1) The oxide must have a slow growth rate.

2) The adherence of the oxide to the substrate must be maintained, even under thermal cycling conditions.

Al_2O_3 is regarded as one of the best oxides for this use. It is a dense oxide, with relatively few ionic defects, and therefore slow-growing. There remains, however, a problem with the adherence of the scale to the alloy to be protected, especially during thermal cycling.

Even under isothermal oxidation conditions stresses develop within an oxide and may cause spallation. These "growth stresses" are impossible to avoid. Pilling and Bedworth[25] have proposed that the change in volume associated with the conversion of metal to oxide is the cause of the stresses and have developed a ratio of volumes that can be used semi-quantitatively to determine the sign and magnitude of the stresses involved. Stringer[26] and Tylecote[27] have, however, asserted that this ratio is not a valid guide to the stresses or adherence of an oxide. Other sources of stress that have been proposed include: stresses due to point defects;[28] growth of new oxide within an already established oxide layer;[29] compositional changes of the oxide near the oxide/alloy interface;[28] recrystallization within the scale at high temperatures in response to growth stresses;[26] and epitaxial stresses near the interface from mismatch of the scale and underlying substrate.[28]

Under conditions of thermal cycling, adherence problems are clearly due to the difference in thermal expansion coefficients for the oxide and underlying substrate. An oxide that is produced in a stress-free state at high temperatures comes under stresses during cooling the magnitude of which can be calculated:[31]

$$\sigma_{ox} = \frac{E_{ox}\,\Delta T\,(\alpha_{ox} - \alpha_m)}{1 + \frac{2E_{ox}}{E_m}\,\frac{t_{ox}}{t_m}}$$

where

σ_{ox} = the stress in the oxide

E_{ox} = the elastic modulus of the oxide

E_m = the elastic modulus of the alloy

ΔT = associated change in temperature

α_{ox} = thermal expansion coefficient of the oxide

α_m = thermal expansion coefficient of the alloy

t_{ox} = oxide thickness

t_m = alloy thickness

In the alloys used in this work the stress created in Al_2O_3 cooled from 1200°C is 35,000 psi.[32]

Of course, when any material is put under high stress, some form of stress relief will occur. In these oxides the stress causes either plastic deformation of the oxide or alloy, or oxide scale failure by cracking and/or spalling.

Oxides are generally brittle materials, though they may show slight plastic behavior at high temperatures.[26,33] Stringer[26] suggests that, instead of plastic flow, oxides experience "stress-directed growth." Douglass[33] concludes that stresses in oxides are accommodated by the developed grain size and scale porosity.

Adherence Improvements by Additions and Dispersions

In the 1940's, in work with Ni-20Cr (Nichrome) for use as a heating element material, the addition of very small (< 0.5%) of yttrium, lanthanum or cerium to Ni-30Cr was found to increase the life of the elements 2970 hours at 1200°C and 613 hours at 1300°C.[34] This improvement was due to a sharp decrease in spallation of the protective Cr_2O_3 during thermal cycling. This phenomenon was referred to as the "Rare Earth Effect," but has since been found to occur with the addition of many elements that have high affinities for oxygen. The improvement also occurs when a dispersion of particles of the oxide of these elements is present in the alloy. Depending on the addition and material, the growth rate of the oxide may also be affected, though this appears to be true only for materials that form Cr_2O_3 as the protective oxide.

In general, the breakaway of the oxide scale is suppressed, leading to a slower oxidation rate of the underlying alloy. The effect seems to be less dramatic with alloys that form Al_2O_3 as the external scale than it is for Cr_2O_3 formers.[35]

For alloys that form Al_2O_3 as the external scale the oxide dispersions improve adherence to a greater degree than the element additions. The dispersion seems to have no effect on the growth rate of Al_2O_3,[36] which probably grows by oxygen diffusing inward along oxide grain boundaries.[37] With scales that grow by metal ions diffusing outward, the dispersions may act as surface nucleation sites for the oxides, reducing the time required for the transient, initial stages of oxidation and reducing the final oxide grain size. With Al_2O_3, however, the dispersion does not affect the transient stage,[38] the oxide grain size already being so small that the dispersion does not alter the internuclei spacing.

Several mechanisms for this improvement in scale adherence have been propposed. None of them differentiate between the presence of an oxide dispersion or element addition. The elements used as additions have very high affinities for oxygen and probably oxidize in preference to chromium and aluminum. Since they are present in very low percentages they therefore would become dispersions of the oxide present as particles within the alloy--just as if they were originally added in that form.

The mechanisms for adherence that have been proposed include:

1) Keying or Pegging.[28,38-42] On several alloys "pegs" of the external oxide grow into the substrate and surround the internal particles. The means by which these pegs improve adherence is strictly a mechanical effect.

2) Vacancy Sink Model.[43] On the alloys with no additions voids are often found to appear at the scale/alloy interface. These voids are thought to be the result of vacancies introduced by the diffusion of metal ions during the production of the oxide scale. These vacancies combine to form the small voids and reduce the area of contact between the scale and alloy.

3) Modification of Scale Plasticity.[44-46] This proposal asserts that the finer-grained oxide produced on an alloy containing an addition/dispersion will more easily accommodate stresses due to a greater grain-boundary area. However, Douglass[35] has found that the presence of particles of Y_2O_3 or $YAlO_3$/$Y_3Al_5O_2$ of the oxide by inhibiting sliding along grain boundaries and decreases the plasticity of the oxide.

4) Graded Seal.[47] It has been proposed that a thin layer of a compound of the oxide addition and protective oxide may exist at the alloy/scale interface and that this layer may have a coefficient of thermal expansion intermediate to the coefficients for the oxide alloy. A layer of this type would provide a degree of stress relief during thermal cycling.

5) Prevention of formation of convoluted oxide morphology.[48] According to this hypothesis Al_2O_3 may grow not only by diffusion of oxygen inward, but also by the diffusion of aluminum outward. At the point where the two species meet, new oxide is formed, leading to large compressive stresses and a convoluted morphology. Perhaps the presence of an addition/dispersion incorporated into the scale would block the diffusion of Al and the need for a convoluted oxide morphology.

6) Chemical Bond.[49] This proposal suggests that chemical bonding forces improve the adherence between the alloy substrate containing the dispersion and the external scale. Investigating this mechanism is one of the aims of this work.

Chemical Bonding Adherence Mechanism

The additions used to improve the adherence of the protective Al_2O_3 layer are elements with high affinities for oxygen--necessarily higher than the oxygen affinities of the other elements present in the alloys. The standard free energy of formation of the dispersion is much more negative than the free energies of the oxides of the other elements present. Consequently, it is possible that the more oxygen-active elements may promote oxide adherence by developing stronger atomic bonds across the oxide/substrate interface.[49] Table III lists the standard free energies of formation (ΔG_f°) for a few important oxides at 1200°C.

Table III

Oxide	ΔG_f° (kcal/mole oxide)	log P_{O_2}
CoO	- 31[50]	- 2.3
Cr_2O_3	-179[50]	-17.7
Al_2O_3	-288[50]	-28.5
HfO_2	-289[51]	-43
Y_2O_3	-314[52]	-31.1
ThO_2	-314[52]	-46.7

The equilibrium partial pressure of oxygen associated with the oxide reacting with its element at 1200°C is also listed.

McDonald and Eberhart[53] concluded that small percentage of a highly oxygen-active metal dissolved in an alloy may play a dominant role in improving oxide adherence by developing stronger atomic bonds across the oxide/substrate interface.

INTRODUCTION TO PRESENT WORK

In order to investigate the validity of the proposed chemical bonding adherence mechanism a situation is set up whereby the oxide used as a dispersion and the oxide used for the protective external scale are identical chemically. In this case, should adherence still be shown to be improved to the same degree by the presence of the dispersion, this mechanism would be invalid.

In this work, a Co-10Cr-1Al alloy is subjected to conditions whereby an Al_2O_3 dispersion forms. The alloy is then aluminized to provide sufficient amounts of aluminum so that a continuous Al_2O_3 film forms when the alloy is oxidized.

As a comparison for oxidation resistance and an alloy for investigating dispersion production, Co-10Cr-11Al and -5Al alloys with hafnium additions are used. During aluminizing treatment very briefly mentioned above, the alloys are exposed to an environment for producing a HfO_2 dispersion and surface aluminide layer at the same time. By controlling the length of treatment the size and distribution of particles should be controlled.

EXPERIMENTAL METHODS

Materials

Table IV gives the nominal compositions of the alloys used in this work. The alloys were prepared by vacuum melting at 1500°C in a inert gas induction furnace. The metals were heated to 1500°C, held for fifteen minutes to insure adequate mixing of the reactive element into the melt, and cast in cylindrical ingots 6-1/2 cm in diameter and 15 cm long. No homogenization treatment was carried out because of the probability of oxidizing the reactive element in the process. This preparation by induction melting produces a rapid stirring motion in the molten bath and avoids the problems of inhomogeneity.[28]

After removal of the outer surface of the ingot on a lathe, the ingots were cut into specimens approximately 1 cm × 1 cm × 0.5 cm using a rotating silicon carbide wheel. All surfaces of each specimen were ground on 180, 320, and 600 grit silicon carbide papers. Specimens were cleaned with acetone and ethyl alcohol in preparation for all treatments.

A typical microstructure found in the materials with 11% aluminum is shown in Figure 2. There are generally two phases present--the cobalt-rich α-solid solution phase, and a darker phase of β-CoAl. The amount of β present is directly proportional to the amount of Al in the alloy. It appears quite prominently in the alloys of 11% Al. Alloys of 5 percent Al are composed mainly of the light phase, and no β appears in a one percent aluminum alloy. After an aluminizing treatment (see below), a layer of the dark phase quite often appears at the

surface of these latter two alloys. In the hafnium-addition alloys, no third phase is seen on micrographs, indicating that hafnium is completely soluble at these concentrations in the alloys. This complete solubility provides the fine dispersions of HfO_2 seen after internal oxidation treatments.

Table IV

Nominal Compositions of the Alloys
(weight %)

Cr	Al	Hf
10	1	
10	5	1.5
10	11	1.0
10	11	0.3

Balance is cobalt in all alloys.

Internal Oxidation Treatment

To provide an internal oxide dispersion of Al_2O_3 in the Co-10Cr-1Al samples, the specimens were encapsulated in a quartz tube with powders of Co-30Cr and Cr_2O_3. The powders and metal samples were kept strictly separate during the process. During final sealing the capsule was heated to 100°C, held for an hour, evacuated to 10^{-5} mm Hg, and sealed off. It was then placed into a larger quartz tube with pieces of tantalum foil. The outer tube was again evacuated and sealed. This "Rhines pack" provides exclusive oxidation of any element present in the alloy having an oxide with a lower oxygen dissociation pressure than the Cr_2O_3. In this alloy the only such element is aluminum

(see Table II). This method of internal oxide production has been used for dilute alloys of copper, nickel, cobalt and iron.[54]

The specimen and capsule were placed into a furnace at 1100°C and kept at temperature for 120 hours. After removal from the furnace and capsule, the specimen surfaces were again ground to 600 grit and cleaned.

Aluminizing Treatment (HfO_2 production)

All specimens were subjected to an aluminizing treatment. Following techniques outlined by Seltzer, Wilcox and Stringer,[55] the specimens were placed into crucibles and surrounded by a mixture of powders of CoAl (49 %), Al_2O_3 (49 %), and NH_4Cl (2 %). This "cementation pack" was then wired shut and placed into a furnace at 1100°C for varying times. Specimens of Co-10Cr-1Al remained at temperature for 162 hours, and specimens containing hafnium were held for 63, 100, or 144 hours. After aluminizing all specimens were annealed in an inert gas furnace for 22 hours.

Aluminizing by this method is done essentially by vapor deposition of aluminum onto the alloy. The CoAl provides the aluminum, the NH_4Cl is an "activator" for the process, and Al_2O_3 provides an inert filler material to prevent sintering of the CoAl particles. The Al is deposited via gaseous transport as $AlCl_3$ or AlCl. For aluminide production on nickel-based alloys the reactions involved, in the temperature range of 750° to 1000°C, have been determined as:[56]

$$Al \text{ (from pack)} + HCl \text{ (activator)} \rightarrow AlCl_3 \text{ (gas)}$$

$$AlCl_3 \text{ (g)} + Ni \text{ (substrate)} + H_2 \text{ (activator)} \rightarrow Ni_2Al_3 + HCl$$

The "activator," NH_4Cl in this case, is obviously an important component to the process. Since it sublimes at 335°C, a sufficient reservoir of it must be maintained by sealing the furnace and/or the pack container.

In the alloys containing hafnium additions, internal oxidation occurred simultaneously with the aluminizing. If these alloys were to be internally oxidized via the "Rhines pack" treatment, the powders added to the pack to lower the oxygen partial pressure would be CoAl and Al_2O_3 (see Table II). Therefore, except for NH_4Cl, the conditions are identical during aluminization, the lowered oxygen pressure is obtained, and hafnium is the only element allowed to oxidize.

Oxidation Experiments

All oxidation experiments were done at 1200°C in an air furnace. Specimens were weighed on an analytic balance and the surface area of each measured with a micrometer previous to all treatments. Three oxidation treatments were done on each alloy: cyclic, short-term isothermal, and long-term isothermal.

Cyclic oxidation experiments were done with eight cycles of twenty hours each. Previous to the first cycle, the specimen was weighed and measured for surface area. The specimen was re-weighed after each succeeding cycle. The treatment was done in recrystallized alumina

crucibles, and the weight of the crucible containing the specimen was the recorded value. The change in mass ($m_i - m_o$) divided by the specimen surface area was then calculated.

The short-term isothermal specimens were left at temperature for 26 hours. Long-term isothermal specimens remained at temperature 344 hours. The specimen surface area was measured before and the mass was recorded before and after the treatments. Change in mass divided by surface area was calculated.

Metallography

Examination of a typical specimen was done after each treatment. Specimens subjected to the internal oxidation and/or aluminizing stages were cleaned by light grinding on 600 grit paper and then mounted in epoxy for polishing and examination with an optical metallograph and scanning electron microscope. X-ray analysis was carried out using an Energy Dispersive Analysis (EDAX) attachment with the SEM.

Oxidation samples were examined various ways. The outer surface of the oxide was examined using the SEM immediately after oxidation. If a region was present where the scale had spalled the oxide fracture surface and the substrate surface under the oxide was examined. The sample was then mounted in epoxy and polished with successively finer diamond pastes to one micron. An examination of the cross section of the oxide-metal interface was made using the metallograph. Much care was taken to avoid excessive destruction of the oxide layer during polishing. Finally, an etchant of Methanol-10% Bromine was used to lightly etch the sample to bring out features of the interface and alloy

grain structure for metallographic examination. The same etchant was then again used to deep-etch the sample to reveal the features of the underside of the oxide at the oxide/metal interface. The SEM was used in examination of this structure.

Before examination using the SEM, all specimens were coated with gold using a gold-sputtering unit. This was done to compensate for the non-conductive properties of the oxides.

RESULTS AND DISCUSSION

INTERNAL OXIDATION AND ALUMINIZING TREATMENTS

METALLOGRAPHY

As indicated in the Introduction to Present Work section, the major objectives of this work were:

(a) to determine whether a fine dispersion of Al_2O_3 particles in a CoCrAl-type alloy (and hence in a CoCrAl-type coating) would be as efficient in improving the adhesion of the Al_2O_3 scale which forms on subsequent high temperature exposure as is an active element (Y, Hf, etc.) or active element oxide dispersion (HfO_2, ThO_2, etc.), thereby eliminating the 'chemical' from the proposed mechanisms; and

(b) to determine whether CoCrAl alloys (and hence coatings) containing metallic Hf additions could be converted to HfO_2 dispersion-containing materials during an aluminizing pretreatment.

In order to achieve the first objective an internal oxidation step, separate from the aluminizing treatment was required. Thus a Co-10Cr-1Al alloy was internally oxidized in a "Rhines pack" as discussed in the Experimental section. Co-10Cr was chosen as the base, since this Cr content is typical of commercially available CoCrAl overlay coatings, and also this level of Cr was used in a previous study[28] of the effects of various active elements and internal oxidation pretreatments on the oxidation of CoCrAl alloys. Of course, after the internal oxidation pretreatment, it was necessary to aluminize the Co-10Cr-1Al alloy, otherwise it would not form an Al_2O_3 scale on subsequent exposure to air or

oxygen.

In relation to the second objective, a CoCrAl, again containing 10% Cr, but now with 11% Al and various levels of Hf was used, which also permitted comparison with previous work. Normally it would not be necessary to aluminize this alloy to ensure formation of an Al_2O_3 scale during subsequent oxidation because the 11% Al is already sufficient. However, simultaneous enrichment of the surface layers of the alloy with Al during internal oxidation would not be anticipated to have a detrimental effect unless the surface became too brittle. In part to counteract this, a Co-10Cr-5Al-Hf alloy was also subjected to similar treatments.

Co-10Cr-1Al

Figure 3 shows this alloy after the internal oxidation treatment only. The internal oxide particles exist in varying shapes, from spherical to rod-like, and are present to a depth of approximately 25 microns. The rod-like shape of some of the particles is apparently due to the diffusion of aluminum outward through the alloy along short-circuit paths and the inward diffusion of oxygen along those same paths. Aluminum at this concentration is in solid solution with the cobalt and chromium, and therefore provides a dispersion of particles throughout the surface region.

Figure 4 shows a Co-10Cr-1Al sample after the internal oxidation and aluminizing treatments. Figure 4 shows the CoAl phase appearing as would be expected from the phase diagram, to a depth of 20 microns, and the depth of internal oxidation has been extended to approximately 50

microns. After etching it is revealed that lower concentrations of Al extend to greater depths. Al is completely soluble in this alloy to approximately 15% according to a Co-Al phase diagram and concentrations below this are indistinguishable, on a light microscope, from pure Co. The increased aluminum contents extends into the alloy 100 microns. It should be noted that Al_2O_3 particles are present within the aluminide layer, indicating that the production of the aluminide layer is accomplished mainly by inward diffusion of the aluminum rather than outward diffusion of cobalt. The apparent further internal oxidation of aluminum is perhaps due to the presence of residual oxygen, at sufficient partial pressure within the cementation pack, during the first hours of the aluminizing treatment.

A Co-10Cr-1Al alloy with only the aluminizing treatement is shown in Figure 5. The darker CoAl phase is present to a depth of 50 microns, and appears to include a region of oxide and porosity approximately 40 microns below the surface. Upon etching, the aluminide layer is revealed to extend no further into the alloy at lower Al contents as in the pre-internally oxidized specimens. Certainly, the Al_2O_3 particles present in the alloy would provide discontinuities in the grain structure of the alloy, and perhaps permit greater short-circuit diffusion of Al into the alloy during aluminization. The region of oxide below the surface of the non-preoxidized specimen is shown by etching to be relatively continuous and may be due to inclusions from the pack during aluminizing. Porosity may also be due to a Kirkendall effect during the aluminizing treatment. This would provide a layer of brittle material near the surface of the alloy and essentially reduce the thickness of the alumnide

layer to 10 microns.

Hafnium-Containing Alloys

A layer of CoAl was also produced on the surface of the hafnium containing alloys. Simultaneously, a dispersion of HfO_2 was produced during aluminizing. The oxygen partial pressure in the aluminizing pack was reduced due to the presence of aluminum and Al_2O_3 to the level shown in Table II. With an inert gas atmosphere outside the pack, this simulates a Rhines pack for internally oxidizing hafnium.

Figures 6 through 8 show the morphology of these alloys after aluminizing for various times. Table IV lists the aluminide layer thickness, particles size and distance between particles for each alloy and aluminizing time.

In each case, the dispersion tends to be basically uniform throughout the alloy, within perhaps a little concentration at grain boundaries. This indicates that hafnium is in solid solution in the basic alloy, and that oxygen diffuses inward to produce the dispersion. Unlike the Al_2O_3 particles in the previous alloys, the HfO_2 particles are not concentrated near the surface of the sample. The internal oxidation process at this low P_{O_2} is limited by oxygen supply at the alloy surface instead of diffusion through the alloy. Therefore, the alloy becomes saturated by oxygen and HfO_2 particles appear throughout the alloy as supersaturation occurs. Undoubtedly there are HfO_2 particles present in a size that is unresolved by the microscopes used. HfO_2 particles are seen in all cases to be present within the aluminide layer, showing that the layer is produced by the inward diffusion of aluminum,

rather than Co diffusing out.

Table IV

Effect of Aluminizing on Hafnium-Containing Alloys

Alloy*	Aluminide layer thickness	HfO_2 particle size	Distance between particles
-11Al-0.3Hf			
63 hours	15 microns	1 micron	30 micron
100	45	1	15
144	45	1	10
-11Al-1Hf			
63	20	2	10
100	25	3	10
144	50	3	10
-5Al-1.5Hf			
63	25	3	10
100	60	3	5
144	70	1	5

*All alloys are Co-10Cr with the given additions.

Continuous regions of oxide and/or porosity are found within the outer parts of the aluminide layer on Co-10Cr-11Al alloys aluminized for longer times limiting the effective aluminide layer thickness.

Due to the fact that Co-10Cr-5Al alloys are one-phase, with only very small concentrations of β-phase in the alloy the aluminide layer addition is more evident in this alloy than in the others. In the etched sample of Figure 8b, energy dispersive x-ray analysis (EDAX) revealed that the oxide near the surface is alumina and that this layer is not continuous as in the lower concentration (Hf) alloys. The small particles dispersed throughout the matrix with some concentration at grain boundaries were analyzed as HfO_2.

Table IV reveals some interesting, although predictable, trends. For all alloys, the aluminide layer thickness seems to increase with aluminizing time. The layer thickness for a given time increases with hafnium content of the alloy, apparently independently of original aluminum content. As with the alloys originally at 1 percent aluminum, this may be due to the discontinuity, and therefore short-circuit diffusion path, presented by the oxide particles. The concentration of the particles obviously increases with hafnium content.

Generally, particle size increases with hafnium content of the alloy. Accordingly, the distance between particles decreases with increasing content. Allam[28] suggested that it is a combination of small oxide particles and fine, uniform dispersion that enhances oxidation resistance and adherence of the scale in these alloys.

RESULTS AND DISCUSSION

OXIDATION EXPERIMENTS

All alloys were subject to three types of oxidation experiments at 1200 °C: Short-term isothermal (26 hours), Cyclic (8 cycles of 20 hours), and Long-term isothermal (344 hours). The relationships between oxidation, oxide production and alloy weight changes will be examined in this section.

METALLOGRAPHY

Co-10Cr-1Al alloys

Short-term oxidation. Illustrations of the effects aluminizing at lower temperatures has on oxidation of these alloys are seen in Figures 9 and 10. The pre-internally oxidized sample in Figure 9 retains some oxide on the surface, though it is not particularly adherent. The metal substrate is bared in several places and higher magnification with EDAX analysis shows the presence of Al_2O_3 particles extending into the substrate and surface imprints from the spalled oxide layer. The underlayer of oxide in Figure 9a consists mostly of aluminum with a small amount of cobalt detected. The outer oxide is pure Al_2O_3. Figure 10 reveals that the alloy with no internal oxidation treatment prior to aluminizing and oxidation is completely oxidized, with consecutive layers (from surface), of pure CoO, a layer of combined oxides of cobalt, aluminum, and chromium, a third layer consisting mostly of Cr oxides with Co present, and in the innermost oxide Co is the predominant element with

some Cr. These oxides are typical of dilute Co-Cr alloys, and apparently the aluminizing treatment has had no effect on this alloy. Both these samples were oxidized only six hours at 1200 °C.

With a more substantial aluminizing temperature at 1100 °C, samples oxidized for 26 hours after internal oxidation and aluminizing treatments did produce and retain the protective Al_2O_3 layer, as shown in Figure 11a. The oxide has a fine-grained structure on the outermost surface, but when this layer spalls, large smooth grains of oxide are revealed. This probably indicates inward diffusion of oxygen during oxide growth. Figure 11b shows an area where all Al_2O_3 has spalled, and the base metal underneath has begun to oxidize. Apparently the aluminum and chromium contents of the substrate are still high enough to prevent the growth of large, columnar grains of CoO.

In some areas, the surface of the non-internally oxidized samples appears identical to the surface seen in Figure 11a. However, this alloy produced CoO upon oxidation for 26 hours over much of the surface. This outward-growing, large-grained oxide is practically non-adherent, and Figure 12 shows evidence that once it begins to grow it destroys any Al_2O_3 scale present.

Cross-sections of these alloys are shown in Figures 13 and 14.

Figure 13a shows an internally-oxidized sample after short-term oxidation. The internal oxide still extends to a depth of approximately 50 microns. The large, smooth Al_2O_3 grains are very evident extending from the alloy surface into the substrate. By etching in stages, different aspects of the interface are revealed after each etch. A 30 second etch shows an external oxide layer approximately 100 microns thick.

After etching 2 minutes, the layer of aluminide is seen to extend 70 microns below the oxide surface. Evidently the aluminum diffuses into the substrate as well as outward to produce the external scale. (This has detrimental effects for longer oxidation times.) A 7 minute etch reveals the underside of the oxide scale. This alloy, with previous internal oxidation treatment, has "pegs" extending from the underside of the scale into the substrate, as Figure 13d shows. The pegs are quite fine and on the order of 15 microns in length after 26 hours of oxidation. The development of these pegs during oxidation has been connected with the presence of internal dispersions, and in this alloy was the reason for a prior internal oxidation treatment. It is the presence of pegs of this kind to which greater adherence of the external oxide scale has been attributed.[28]

Figure 14a has a cross-section of the same alloy with no prior internal oxidation treatment. These pictures were taken in a region where Al_2O_3 is the external scale. Some "pegging" is present, but it is the exception rather than the rule. An outer, continuous layer of oxide is present. However, this layer has broken away from the substrate. After a 2 minute etch the oxide layer and aluminide near the surface can be seen. This aluminide layer after 26 hours of oxidation extends some 40 microns below the surface, and aluminum does not seem to be diffusing inward at too great a rate. A seven minute etch in Figure 14c shows the underside of the oxide to be basically free from pegs and large-grained.

The presence of internal oxide particles not only seems to enhance oxidation resistance, it also promotes the diffusion of Al into

the alloy during aluminization. This, in turn, assists in an even greater resistance to oxidation by providing more Al needed to restore the protective scale after spalling.

Cyclic oxidation. Cyclic oxidation produced dramatic differences in the two types of 1 percent Al alloys. The alloy with the internal oxide dispersion has a much more abundant supply of Al to rebuild spalled oxides and a much more adherent scale. Figure 15 shows the layer of Al_2O_3 at a spalled area. Only a small area of metal is bared, and evidence of the underlying internal oxide can be seen.

An interesting effect of cyclic oxidation on this alloy appears near the alloy surface where the aluminide layer was prior to oxidation. Due to the diffusion of Al during oxidation, a layer near the surface of the alloys begins to develop the two distinct phases seen in the 11Al alloys. The interior of the specimen, however, remains one-phase. This effect would eventually lead to CoO growing over the Al-depleted regions.

The 1% Al alloy with no internal oxidation was completely oxidized with a thick surface layer of CoO after only 3 cycles. A comparison of the weight changes of these samples during cyclic oxidation experiments is found in the Kinetics part of this section.

Long-term oxidation. Both of thhe Co-10Cr-1Al types of alloys were completely oxidized after 344 hours at 1200 °C, and covered with a layer of CoO.

Hafnium-containing Alloys

For purposes of comparison, an alloy of composition Co-10Cr-5Al was subjected to the oxidation experiments. No internal oxide is present and with no aluminizing treatment this alloy is completely vulnerable to rapid oxidation.

Short-term oxidation. After short-term oxidation the surface of an alloy of 5Al that has been aluminized 63 hours appears as in Figure 16a. There are layers of oxides containing a high percentage of aluminum on the surface, but at high magnification (Figure 16b) the reason for the brittleness of the oxide and its inability to protect the alloy underneath can be seen. The oxide is an extremely porous structure, evidently because of insufficient aluminum available to produce a dense layer of Al_2O_3. With a longer aluminizing time of 144 hours Al_2O_3 covers most of the surface, though it is still not continuous.

A view of the top of the second oxide layer on a 5Al alloy aluminized 63 hours shows (Figure 16c) a reason for adherence problems. Voids exist at the interface, with a corresponding loss of contact, leading to loss of adherence. Aluminum vapor pressure inside the void at this high temperature is high enough to supply Al to the oxide underside, maintaining its growth even though it is not in contact with the alloy. This vaporization of aluminum causes the smooth walls of the void.[28]

Oxidation for 26 hours of a Co-10Cr-5Al-1.5Hf alloy produces a more continuous, finer-grained oxide than the same alloy with no hafnium. Without aluminizing the oxide produced is identical to that of a dilute

Co-Cr alloy with no aluminum or hafnium, and spalls easily. As the alloy is aluminized for longer times, a greater percentage of the oxide produced is Al_1O_3. An aluminizing time of 63 hours gives a continuous layer of oxide, mostly Al_2O_3. The oxide structure on this alloy aluminized 100 hours resembles that found on the alloys of Co-10Cr-1Al-large, smooth grains beneath a layer of fine surface oxide. All the oxide present is Al_2O_3. With 144 hours of aluminizing, the oxide produced is nearly continuous and all Al_2O_3 (Figure 17a). There seems to be a ready supply of Al in this alloy for further oxide production.

A cross-sectional view of this alloy after 100 hours aluminizing and short-term oxidation is shown in Figure 17b. The β layer extends to the surface, and no pegs are present. A region of metal bared after spallation of the oxide of the alloy aluminized 100 hours is shown in Figure 17c. The oxide imprints left behind are small, on the order of one micron in diameter and no voids are present. The Al_2O_3 layer appears to be quite adherent.

Alloys of 11% Al content can produce a continuous Al_2O_3 layer. Additional aluminizing may embrittle the surface material. Co-10Cr-11Al-0.3Hf oxidized for 26 hours produces a surface oxide layer as shown in Figure 18a. If the oxide spalls, there is sufficient aluminum to reform the scale. With 63 hours of aluminizing the oxide surface is fine grained and still apparently adherent. However, further increases in aluminizing time begin to cause voids to form under the scale during oxidation. Voids on samples aluminized 144 hours are shown in Figure 18b. The smooth surfaces of the substrate and large grains on the

underside of the oxide indicate that within the void the pressure at this temperature during oxidation is low enough to allow aluminum from the substrate to be vaporized and provide a relatively fast supply of Al to the oxide layer. The large grains of oxide grow, unrestricted by a growth-retarding substrate.[28] Of course, the presence of these voids means a loss of adherence locally at the alloy/oxide interface.

In some areas the voids may not be present, but still the oxide is not completely adherent. In Figure 18c the oxide of the alloy with no aluminizing treatment is seen from the underside after loosening. The imprints on the substrate appear to match the grain structure on the oxide underside. This spalling was probably due to stresses produced during cooling.

Figure 18d shows the microstructure of the alloy after aluminizing for 63 hours and short-term oxidation. The surface layer of aluminide is being depleted. The aluminide layer now extends deeper into the substrate. These two facts indicate the Al is diffusing away from the surface region both outward to produce Al_2O_3 on the surface and inward to regions of lower aluminum content.

No evidence of pegging was found in cross-sections of this alloy. However, Figure 18e shows the broken-off top of a peg of Al_2O_3 that extends into the alloy.

Figure 19a shows a typical surface morphology for oxidized samples of Co-10Cr-11Al-1Hf that have been aluminized. Samples aluminized 63 or 100 hours tend to have comparable coverage of Al_2O_3. When the oxide does spall there is sufficient Al in thhe substrate to replace

it. Samples aluminized 144 hours also have sufficient Al, but spalling is much more common and the oxide is finer-grained.

The microstructure of Co-10Cr-11Al-1Hf aluminized for 63 hours and then oxidized is shown in Figure 19b. The same alloy with no aluminizing has pegs 20 microns long and with quite a fine dispersion, and the surface is depleted of β phase. The abundance of pegs seems to decrease with aluminizing time, and pegs appear only within areas of pure α. The depth of the aluminide layer markedly increases with oxidation indicating again that Al is diffusing deeper into the alloy as well as to the surface for Al_2O_3 production.

Figure 19c shows a typical substrate surface on these alloys after spallation of the oxide. The oxide grains at the inner surface of the oxide are larger than those on the outer surface. Imprints on the substrate are on the order of 10 microns in diameter—larger than those found on the Co-10Cr-11Al-0.3Hf alloy surface under the oxide.

Cyclic oxidation. The completely non-adherent oxide scale produced on a Co-10Cr-5Al alloy during cyclic oxidation is shown in Figure 20. Large columnar grains of CoO are outermost, with brittle a oxide of Co and Al between the CoO and the substrate.

The oxide surface of Co-10Cr-5Al-1.5Hf aluminized 100 hours and subjected to cyclic oxidation is shown in Figure 21a. Specimens aluminized 100 hours have oxides of pure Al_2O_3, though they are not smooth oxides. Upon spallation more Al_2O_3 is produced. Sixty-three hours of aluminizing does not produce a large enough reservoir of Al to withstand cyclic oxidation, and by the end the oxide is a fine-grained mix of Co

and Al. The oxide on the specimens aluminized 144 hours is very broken and easily spalled, presumably due to the high Al and HfO_2 contents of this alloy.

The microstructure of this alloy is shown in Figure 21b. The sample aluminized 100 hours still retains its aluminide layer for Al_2O_3 production, though larger pegs are produced which may lead to loss of oxide adherence. The aluminide layer has penetrated to a greater depth and the surface is being depleted of Al. While the sample, when aluminized 63 hours, produces many oxide pegs, the aluminum content of the alloy is very low after cyclic oxidation. No aluminide layer remains, and upon spallation Co oxides are produced. The sample aluminized 144 hours has very large oxide pegs that are probably the reason for the loss of scale adherence.[28]

The oxide surface of Co-10Cr-11Al-0.3Hf aluminized 100 hours after cyclic oxidation is seen in Figure 22a. The sample aluminized 63 or 100 hours spalled during oxidation and the alloy beneath oxidized in the fine grains of the Co and Al oxide region of Figure 20. Figure 22b, the oxides produced on a sample aluminized 144 hours, shows the oxide layers shown to be typical for the 11% Al alloys in a previous work.[28] The layers have greater aluminum content as they near the outer surface and appear to be adherent to the substrate below.

A microstructure of these samples is shown in Figure 22c. The sample aluminized 63 hours has a depleted aluminide layer, the CoAl is still present near the surface. The sample, when aluminized 144 hours retains its aluminide layer to a depth of 100 microns. The Al is

diffusing into the alloy and out to the surface. No oxide pegs were evident. However, Figure 22d shows that HfO_2 exists throughout the aluminide layer. In this etched sample the oxide underside appears smooth.

Figure 22e shows voids again existing at the oxide/alloy interface in the alloy aluminized 144 hours.

Alloys of Co-10Cr-11Al-1Hf subjected to cyclic oxidation are shown in Figure 23. Figure 23a shows the oxide surface found to be typical of these alloys. There is a continuous underlayer of Al_2O_3 and anywhere spallation occurs enough Al is present to reform the protective oxide. Oxide pegs, as shown in Figure 23b are very common in the alloys. Again, peg production seems to decrease with increasing aluminizing time, but is still present in the alloy aluminized 144 hours. Figure 23c is a view of the broken-off pegs still in the alloy. Between the two large pegs there is a hole in the substrate where another peg has been removed.

Long-term oxidation. Figure 24a shows the surface oxide scale typically found on a 5% Al alloy, aluminized 144 hours, after 344 hours of isothermal oxidation. The oxide layers are mainly Al_2O_3, but the large imprints on the substrate show a large number of voids and a loss of adherence between alloy and oxide. Figure 24b shows the metal surface of the same alloy aluminized only 100 hours and the evidence of large voids found there.

The 5% Al alloy with 1.5% Hf and aluminized for 63 hours does not resist long-term oxidation. The oxides produced are identical to those of the alloy with Hf addition, subjected to cyclic oxidation as shown in Figure 20 though they appear to be more adherent. However, after being aluminized 100 hours, sufficient Al has been provided and the oxide shown in Figure 25a is produced. The oxide produced on the alloy aluminized 144 hours is much finer-grained.

Figure 25b illustrates how the production of CoO on the alloy destroys the surface. The large grains of CoO are at the original surface, and a brittle oxidized region of mostly chromia and alumina is beneath it. The entire oxide thickness is as much as 2 millimeters thick.

An etched cross-section of this alloy aluminized 100 hours prior to long-term oxidation is shown in Figure 25c. Hafnia particles are abundant with the alloy and oxide pegs are seen extending through the aluminide layer. When the alloy has been aluminized 144 hours the pegs are quite large. Figures 25d and e show a cross-section of the alloy and a region of broken-off peg respectively. Figure 25e shows a region of metal bared next to where the peg enters the substrate. This peg is approximately ten microns in diameter, like those found in Figure 25d.

Alloys of 11Al-0.3Hf contents subjected to long-term oxidation are shown in Figure 26. Figure 26a shows a typical surface of the sample. This sample was aluminized 100 hours and experienced spalling on cooling after oxidation. A sample that was aluminized 63 hours (Figure 26b) shows broken pegs at a spalled oxide area. However, a void

10 microns in diameter at the oxide/alloy interface of a sample aluminized 100 hours is shown in Figure 26c and probably was the cause of local spalling.

Etched cross-sections of these samples are shown in Figures 26d through f. An etched sample of the alloy aluminized 63 hours shows an oxide underside that is nearly devoid of pegs. The aluminide layer is approximately 20 microns thick and aluminum has therefore diffused slightly inward during oxidation. HfO_2 particles are dispersed throughout the substrate. A sample aluminized 100 hours still has only minor irregularities present on the underside of the Al_2O_3. The region of higher Al content on a sample aluminized 144 hours prior to oxidation can be seen in Figure 26f to be now 70 microns thick.

Alloys of 11% Al-1% Hf content produce the oxide surface layer seen in Figure 27a during 344 hours of oxidation. Upon spalling more Al_2O_3 is produced and very little metal bared.

The underside of the oxide produced when a sample of 11Al-1Hf aluminized 100 hours is subject to long-term oxidation is shown in Figure 27b. There are thick pegs extending into the alloy. The small "chunks" evident on them are HfO_2 particles that are enveloped during peg growth. The alloy surface under the oxide is seen in Figure 27c. The oxide imprints are on the order of 10 microns in size. Broken pegs are imbedded in the substrate surface.

RESULTS AND DISCUSSION

KINETICS

The weight change experienced by each alloy during isothermal oxidation experiments is listed below. Figures 28 through 32 show the weight change as the alloys underwent cyclic oxidation.

Table V

Short term isothermal oxidation (26 hours, 1200°C)

Alloy*	$\Delta m/A$ (g/cm^2)
-11Al-0.3Hf Aluminized 144 hrs.	0.0007
-5Al Aluminized 100 hrs.	0.0007
-11Al-1Hf Aluminized 144 hrs.	0.0009
-5Al Aluminized 63 hrs.	0.0009
-11Al-1Hf Aluminized 100 hrs.	0.0011
-11Al00.3Hf As cast	0.0012
-5Al-1.5Hf Aluminized 144 hrs.	0.0013
-5Al Aluminized 144 hrs.	0.0015
-1Al, Internally oxidized 120 hrs, Aluminized 162 hrs.	0.0015
-5Al-1.5Hf Aluminized 100 hrs.	0.0017
-11Al-0.3Hf Aluminized 100 hrs.	0.0018
-5Al-1.5Hf As cast	0.0029
-11Al-1Hf As cast	0.0035
-5Al As cast	0.0083
-1Al Aluminized 162 hrs.	0.0422

*All alloys contain Co-10Cr with the additions shown.

Table V ranks the alloys in order of reducing resistance to short-term oxidation. For this short time of oxidation, most alloys contained enough aluminum to prevent drastic oxidation. All alloys listed down to -11Al-1Hf As Cast showed no evidence of CoO after oxidation. The alloys of -5Al and the -1Al specimen with no internal oxide dispersion did produce CoO.

Table VI

Long-term isothermal oxidation (344 hours at 1200 C)

Alloy*		m/A (g/cm^2)
-11Al-0.3Hf	Aluminized 144 hrs.	negligible
-11Al-0.3Hf	Aluminized 63 hrs.	0.0011
-11Al-1Hf	Aluminized 63 hrs.	0.0013
-11Al-1Hf	Aluminized 100 hrs.	0.0025
-5Al-1.5Hf	Aluminized 144 hrs.	0.0038
-5Al-1.5Hf	Aluminized 100 hrs.	0.0066
-5Al	Aluminized 144 hrs.	0.0243
-11Al-1Hf	Aluminized 144 hrs.	0.0253
-5Al-1.5Hf	Aluminized 63 hrs.	0.0480
-5Al	Aluminized 100 hrs.	0.160
-1Al	Internally oxidized 120 hrs, Aluminized 162 hrs.	0.224
-5Al	Aluminized 63 hrs.	0.589
-1Al	Aluminized 162 hrs.	---

*All alloys contain Co-10Cr with the additions shown.

Table VI lists the weight-change experienced by each alloy after 344 hours of isothermal oxidation. The reactions vary from that of -11Al-0.3Hf aluminized 144 hours experiencing very little weight change to -1Al with only aluminizing treatment falling completely apart. All alloys down to -5Al-1.5Hf aluminized 100 hours produced no CoO. Those below produced CoO in amounts varying from oxidation at the edges of the specimen to complete oxidation.

Cyclic Oxidation

Figures 28 through 32 are graphs of alloy weight changes during cyclic oxidation.

Figure 28 shows weight changes of alloys with no hafnium additions. The alloy of 1% Al with no internal oxidation completely deteriorated in the first cycle. After being aluminized 63 hours the-5Al alloy experienced a minimal weight gain during the first cycle, then suddenly lost its supply of aluminum to replenish spalled Al_2O_3 and oxidized quickly. The same alloy oxidized 100 hours and 144 hours began to oxidize quickly after the first few cycles.

The Co-10Cr-1Al alloy internally oxidized and aluminized did much better than any of the others in the long-run. During initial cycles it experienced a relatively rapid weight gain, but tended to gain weight slower at longer cycles. While the indication of oxidation resistance illustrated here does not approach that of the alloys containing hafnium used in this work, it does compare favorably with alloys containing other additions. For instance, the same alloy with -11Al-1Ce, internally oxidized under nearly identical conditions, does

not resist cyclic oxidation as well as this alloy. It also compares well with the same alloy containing -11Al-0.1Hf with or without prior internal oxidation.[28]

According to Figure 29, Co-10Cr-5Al-1.5Hf alloys are at an optimum aluminizing time at 100 hours. Without aluminizing the alloy does not at all resist oxidation, and both 63 hours and 144 hours of aluminizing produce less resistance to cyclic oxidation than 100 hours. Presumably this is due to a point of optimum aluminum content in the alloy and optimum HfO_2 particle size and dispersion.

From Figure 30 it can be deduced that Co-10Cr-11Al-0.3Hf alloys resist cyclic oxidation better with little or no aluminizing, though after eight cycles samples with 144 hours of aluminizing seem to benefit from their higher aluminum contents.

Alloys with -11Al-1Hf content seem to have optimum aluminizing times of approximately 63 to 100 hours. Both long-term and no aluminizing treatments have less beneficial effects. This is shown in Figure 31.

Figure 32 is a comparison of the cyclic oxidation resistance of the best sample of each alloy. From those present it is obvious that shorter aluminizing times produce alloys most resistant to cyclic oxidation.

SUMMARY AND CONCLUSIONS

The two major conclusions that can be drawn from this work are:

1) An internal dispersion of Al_2O_3 in an alloy that forms Al_2O_3 as a protective scale will improve adherence to a degree comparable to that obtained with certain other dispersions under short-term and cyclic oxidation conditions. This improvement in adherence is a pure mechanical effect due to the formation of pegs in the presence of the Al_2O_3 dispersion, and cannot be due to a chemical bond between the dispersion and oxide scale.

2) Aluminizing an alloy containing a small percentage of hafnium in a "cementation pack" does produce a HfO_2 dispersion. This combination of aluminizing and dispersion may or may not improve adherence of an Al_2O_3 protective scale.

A general summary of other conclusions reached:

In alloys with an Al_2O_3 dispersion:

1) The depth of aluminizing is promoted by the presence of the dispersion during oxidation.

2) Oxide pegs are produced due to the presence of the dispersion during oxidation.

In alloys containing Hf additions:

1) The depths of aluminizing is promoted by increased Hf content and increased aluminizing times.

2) Particle size and dispersion increase with Hf content.

3) Too much aluminizing can embrittle the surface layer of an alloy, resulting in no substrate accommodation of stresses and loss of adherence.

4) There is an optimum degree of aluminizing to produce an HfO_2 dispersion and increase the Al content of the alloy surface.

5) Al_2O_3 pegs form within the α-phase surface region of hafnium-containing alloys. Their formation may not be compatible with aluminization to produce HfO_2, due to the fact that the β-phase then covers the surface.

6) During oxidation aluminum is also diffusing into the base alloy and surface regions may become depleted of necessary aluminum.

REFERENCES

1. W. H. Sharp, "High Temperature Materials II," Proceedings of a Technical Conference, Cleveland, Ohio, April 1961. Metallurgical Society Conference, Vol. 18, John Wiley & Son.
2. G. C. Wood, Werks. Und Korr., 6 (1971) 491.
3. F. D. Richardson and J. M. E. Jeffes, J. Iron and Steel Inst., 160 (1948) 261.
4. O. Kubaschewski and B. E. Hopkins, "Oxidation of Metals and Alloys," Butterworth, London (1967).
5. G. R. Wallwark and A. Z. Hed. Oxid. Metals, 3 (1971) 171.
6. D. L. Douglass and J. S. Armijo, Oxid. Metals, 3 (1971) 185.
7. H. G. Graham and H. H. Davis, J. Amer. Ceram. Soc., 54 (1971) 89.
8. P. K. Kofstad and A. Z. Hed, Werks. Und Korr., 11 (1970) 894.
9. C. E. Lowell and H. B. Probst, NASA TN D-7705, (Aug. 1974).
10. W. C. Hazel, Corrosion, 21 (1965) 316.
11. G. C. Wood and F. H. Stott, Oxid. Metals, 3 (1971) 365.
12. C. Wagner, J. Electrochem. Soc., 99 (1952 369.
13. C. Wagner, J. Electrochem. Soc., 103 (1956) 571, 617.
14. C. Wagner, Corros. Science, 5 (1965) 751.
15. G. C. Wood, Oxid. Metals, 2 (1970) 11.
16. G. C. Wood, I. G. Wright, T. Hodgkiess and D. P. Whittle, Werks. Und Korr., 21 (1970) 900.

17. G. N. Irving, J. Stringer and D. P. Whittle, Oxid. Metals, 9 (1975) 427.

18. N. R. Lindblad, Oxid. Metals, 1 (1969) 143.

19. R. Kosak and R. A. Rapp, 3rd Interamerican Conf. Materials Tech., Rio de Janeiro (1972) 813.

20. A. U. Seybolt, Trans. AIME 1955 (1968) 242.

21. I. G. Wright, Oxidation of Fe-, Ni-, Co-Base Alloys, Metals and Ceramics Information Center Report No. 72-07 (June 1972) 19.

22. G. C. Wood, Oxid. Metals, 2 (1970) 11.

23. G. R. Wallwark and A. Z. Hed, Oxid. Metals, 3 (1971) 171, 213.

24. D. P. Whittle and J. Stringer, "Improvements in High Temperature Resistance by Additions of Reactive Elements or Oxide Dispersions", International Conference on Residuals, Additives and Materials Properties, The Royal Society, London (May 15-17, 1978).

25. N. B. Pilling and R. E. Bedworth, J. Inst. Metals, 29 (1923) 529.

26. J. Stringer, Corros. Sci., 10 (1970) 513.

27. R. F. Tylecote, J. Iron and Steel Inst., Aug. (1960) 380.

28. I. M. Allam, "The Effect of Reactive Element Additions and Oxide Dispersions on Al_2O_3-Scale Adherence", Ph.D. thesis, University of Liverpool, England (January 1978).

29. W. Jaenicke, S. Leistikow and A. Stadler, J. Electrochem. Soc., 111 (1964) 1031.

30. F. N. Rhines and J. S. Wolf, Metall. Trans., 1 (1970) 1701.

31. G. D. Oxx, Prod. Eng., 17 (1958) ¢!.

32. J. D, Kunzly and D. L. Douglass, Oxid. Metals, 8 (1974) 139.

33. D. L. Douglass, Ref. (28), p. 27.

34. A. Raman, Z. Metallkde., 3 (1977) 163.

35. A. Kumar, M. Nasrallah and D. L. Douglass, Oxid. Metals, 8 (1974) 227.

36. C. S. Giggins and F. S. Pettit, Final Report to Aerospace Research Laboratories, Wright-Patterson Air Force Base, Air Force System Command, USAF, Contract F 33615-72-C-1702 (1975).

37. J. K. Tien and F. S. Pettit, Met Trans., 3 (1972) 1587.

38. J. Stringer, Werks. Und Korr., 9 (1972) 747.

39. J. M. Francis and W. H. Withlow, Corros. Sci. 5 (1965) 701.

40. C. S. Wukusick and J. F. Collins, Mater. Res. Stand., 4 (1964) 637.

41. E. J. Felten, J. Electrochem. Soc., 108 (2961) 490.

42. B. Lustman, Trans. AIME, 188 (1950) ((%.

43. J. Stringer, Met. Rev. 11, (1966) 113.

44. J. M. Francis and J. A. Juston, Corros. Sci., 8 (1968) 445.

45. F. S. Pettit, AGARD-CP-120, (1972 155.

46. J. E. Antill and K. A. Peakall, J. Iron and Steel Inst., Nov. (1967) 1136.

47. H. Pfieffer, Werks. Und. Korr., 8 (1957) 574.

48. F. A. Golightly, F. H. Scott and G. C. Wood, Oxid. Metals, 10 (1976) 163.

49. J. K. Tien and F. S. Pettit, Met. Trans., 3 (1972) 1587.

50. Dow Chemical Company, USA, JANAF THERMOCHEMICAL DATA (1978).

51. K. Pitzer and L. Brewer, Thermodynamics (1961) 676.

52. Chemical Rubber Company (CRC), Handbook of Chemistry and Physics (1973) D-45, D-61.

53. J. E. McDonald and J. G. Eberhart, Trans. TSM. AIME, 223 (1965) 512.

54. R. A. Rapp, Corrosion-National Association of Corrosion Enginners, 21 (1965) 382.

55. M. S. Seltzer, B. A. Wilcox and J. Stringer, Met. Trans., 3 (1972) 2391.

56. D. H. Boone, C. G. Giggins, G. W. Goward, E. H. Randlev; Pratt and Whitney Aircraft Report No. 65-020 (1965).

FIGURE CAPTIONS

Figure 1. Oxide map for the Ternary System Co-Cr-Al at 1100°C[23]

Figure 2. Co-10Cr-11Al-1Hf: Interior cross-section
As Cast condition
×760

Figure 3. Co-10Cr-1Al: Surface cross-section
Internally oxidized 120 hrs, 1100°C
Etched 1 minute
×1000

Figure 4. Co-10Cr-1Al: Surface cross-section
Internally oxidized 120 hrs, 1100°C
Aluminized 162 hrs, 1100°C
×920

Figure 5. Co-10Cr-1Al: Surface cross-section
Aluminized 162 hrs, 1100°C
×620

Figure 6a. Co-10Cr-11Al-0.3Hf: Surface cross-section
Aluminized 100 hrs, 1100°C
×1000

6b. Interior cross-section
×840

Figure 7a. Co-10Cr-11Al-1Hf: Surface cross-section
Aluminized 63 hrs, 1100°C
×1000

7b. Interior cross-section
×840

Figure 8a. Co-10Cr-5Al-1.5Hf: Surface cross-section
Aluminized 144 hrs, 1000°C
×760

8b. Surface cross-section, etched 7 minutes
×1000

Figure 9a. Co-10Cr-1Al: Alloy surface
Internally oxidized 120 hrs, 1100°C
Aluminized 150 hrs, 1000°C
Oxidized 6 hrs, 1200°C
×200

9b. Substrate surface
×2000

9c. EDAX X-ray Map (Aluminum)

Figure 10. Co-10Cr-1Al: Sample surface
Aluminized 150 hrs, 1000°C
Oxidized 6 hrs, 1200°C
×20

Figure 11a. Co-10Cr-1Al: Oxide surface
Internally oxidized 120 hrs, 1100°C
Aluminized 162 hrs, 1100°C
Oxidized 26 hrs, 1200°C
×500

11b. Alloy surface under oxide
×1000

Figure 12. Co-10Cr-1Al: Oxide surface
Aluminized 162 hrs, 1100°C
Oxidized 26 hrs, 1200°C
×1000

Figure 13a. Co-10Cr-1Al: Surface cross-section

Fig. 13a (continued)

Internally oxidixed 120 hrs, 1100°C
Aluminized 162 hrs, 1100°C
Oxidized 26 hrs, 1200°C
×1000

13b. Surface cross-section, etched 30 seconds
×180

13c. Surface cross-section, etched 2 minutes
×580

13d. Oxide underside, etched 7 minutes
×1000

Figure 14a. Co-10Cr-1Al: Surface cross-section
Aluminized 162 hrs, 1100°C
Oxidized 26 hrs, 1200°c
×2000

14b. Surface cross-section, etched 2 minutes
×500

14c. Surface cross-section, etched 7 minutes
×1000

Figure 15. Co-10Cr-1Al: Oxide surface
Internally oxidized 120 hrs, 1100°C
Cyclic oxidation, 1200°C
×5000

Figure 16a. Co-10Cr-5Al: Sample surface
Aluminized 63 hrs, 1100°C
Oxidized 26 hrs, 1200°C
×200

16b. Oxide surface
×5000

16c. Voids at alloy/oxide interface
×5000

Figure 17a. Co-10Cr-5Al-1.5Hf: Oxide surface
Aluminized 144 hrs, 1100°C
Oxidized 26 hrs, 1200°C
×200

17b. Surface cross-section
Aluminized 100 hrs, 1100°C
Oxidized 26 hrs, 1200°C
×680

17c. Alloy surface exposed at spalled area
×5000

Figure 18a. Co-10Cr-11Al-0.3Hf: Oxide surface
Oxidized 26 hrs, 1200°C
×440

18b. Voids under oxide
Aluminized 144 hrs, 1100°C
Oxidized 26 hrs, 1200°C
×2000

18c. Spalled oxide/underside
Oxided 26 hrs, 1200°C
×4400

Figure 18d. Co-10Cr-11Al-0.3Hf: Surface cross-section
Aluminized 63 hrs, 1100°C
Oxidized 26 hrs, 1200°C
×1000

18e. Broken off pegs in substrate
×5000

Figure 19a. Co-10Cr-11Al-1Hf: Oxide surface
Aluminizied 100 hrs, 1100°C
Oxidized 26 hrs, 1200°C
×500

19b. Surface cross-section
Aluminized 63 hrs, 1100°C
Oxidized 26 hrs, 1200°C
×680

19c. Oxide/alloy surface
Aluminized 100 hrs, 1100°C
Oxidized 26 hrs, 1200°C
×5000

Figure 20. Co-10Cr-5Al: Oxide surface
Aluminized 100 hrs, 1100°C
Cyclic oxidation, 1200°C
×50

Figure 21a. Co-10Cr-5Al-1.5Hf: Oxide surface
Aluminized 100 hrs, 1100°C
Cyclic oxidation, 1200°C
×200

21b. Surface cross-section
×680

Figure 22a. Co-10Cr-11Al-0.3Hf: Sample surface
Aluminized 100 hrs, 1100°C
Cyclic oxidation, 1200°C
×500

22b. Oxide layers
Aluminized 63 hrs, 1100°C

Fig. 22b (continued)

Cyclic oxidation, 1200°C
×5000

22c. Surface cross-section
Aluminized 63 hrs, 1100°C
Cyclic oxidation, 1200°C
×1000

Figure 22d. Co-10Cr-11Al-0.3Hf: Surface cross section, etched 1 minute
Aluminized 63 hrs, 1100°C
Cyclic oxidation, 1200°C
×500

22e. Voids at alloy/oxide interface
Aluminized 144 hrs, 1100°C
Cyclic oxidation, 1200°C
×4800

Figure 23a. Co-10Cr-11Al-1Hf: Oxide surface
Cyclic oxidation, 1200°C
×500

23b. Surface cross-section, etched 7 minutes
×500

23c. Broken pegs in substrate
Aluminized 100 hrs, 1100°C
Cyclic oxidation, 1200°C
×5000

Figure 24a. Co-10Cr-5Al: Sample surface
Aluminized 144 hrs, 1100°C
Oxidized 344 hrs, 1200°C
×50

Fig. 24 (continued)

24b. Alloy surface
Aluminized 100 hrs, 1100°C
Oxidized 344 hrs, 1200°C
×1000

Figure 25a. Co-10Cr-5Al-1.5Hf: Oxide surface
Aluminized 100 hrs, 1100°C
Oxidized 344 hrs, 1200°C
×920

25b. Surface cross-section
Aluminized 63 hrs, 1100°C
Oxidized 344 hrs, 1200°C
×40

25c. Surface cross-section, etched 7 minutes
Aluminized 100 hrs, 1100°C
Oxidized 344 hrs, 1200°C
×520

Figure 25d. Co-10Cr-5Al-1.5Hf: Surface cross-section
Aluminized 144 hrs, 1100°C
Oxidized 344 hrs, 1200°C
×600

25e. Broken peg with metal exposed
×2000

Figure 26a. Co-10Cr-11Al-0.3Hf: Oxide surface
Aluminized 100 hrs, 1100°C
Oxidized 344 hrs, 1200°C
×500

Fig. 26 (continued)

26b. Oxide/metal surface
Aluminized 63 hrs, 1100°C
Oxidized 344 hrs, 1200°C
×1000

26c. Voids at alloy/oxide interface
Aluminized 100 hrs, 1100°C
Oxidized 344 hrs, 1200°C
×5000

Figure 26d. Co-10Cr-11Al-0.3Hf: Oxide underside (etched 7 min
Aluminized 63 hrs, 1100°C
Oxidized 344 hrs, 1200°C
× 1100

26e. Surface cross-section, etched 7 minutes
Aluminized 100 hrs, 1100°C
Oxidized 344 hrs, 1100°C
×1000

26f. Surface cross-section, etched 7 minutes
Aluminized 144 hrs, 1100°C
Oxidized 344 hrs, 1200°C
×300

Figure 27a. Co-10Cr-11Al-1Hf: Oxide surface
Aluminized 100 hrs, 1100°C
Oxidized 344 hrs, 1200°C
×200

27b. Oxide underside/pegs, etched 7 minutes
Aluminized 344 hrs, 1200°C
Oxidized 344 hrs, 1200°C
×920

27c. Metal surface with broken pegs
Aluminized 144 hrs, 1100°C
Oxidized 344 hrs, 1200°C.
×5000

Figures 28 through 32.

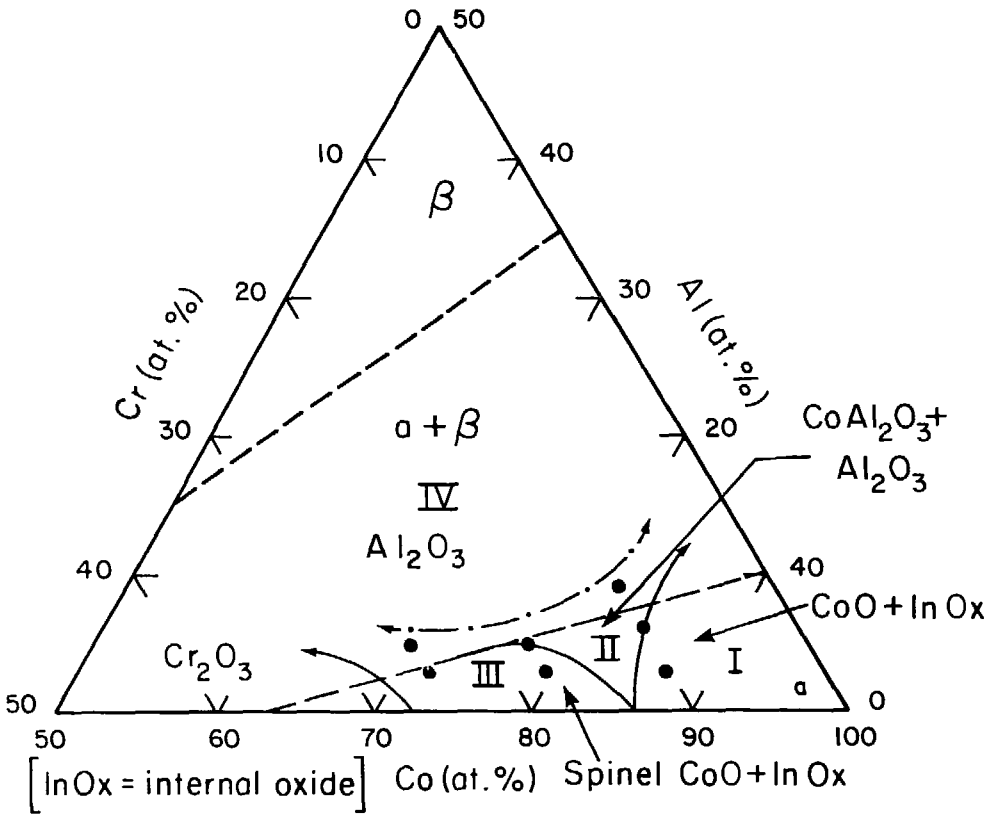

Fig. 1

XBL805-1086

Fig. 2

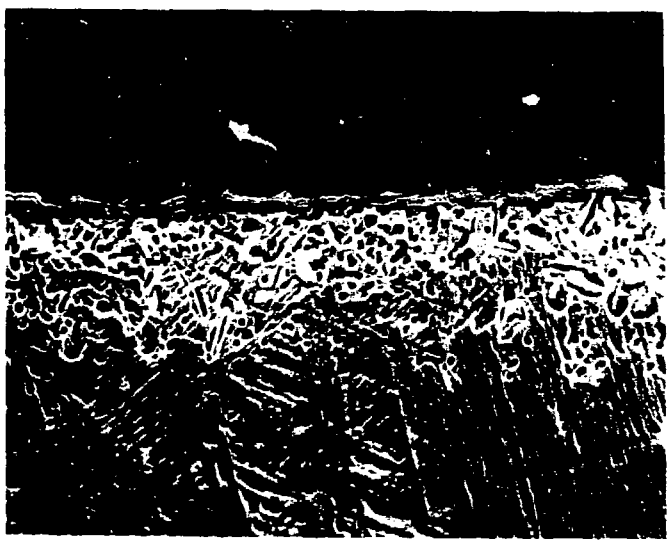

Fig. 3 XBB 805-6889

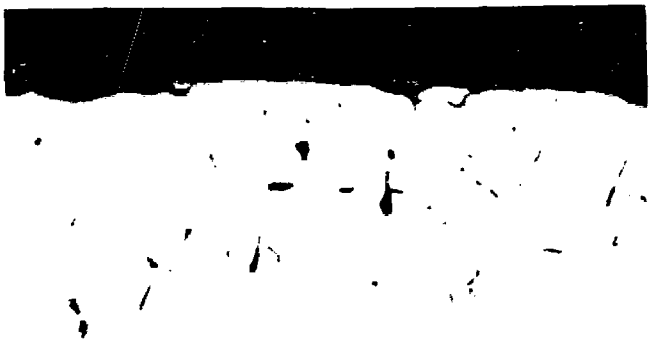

Fig. 4

Fig. 5

XBB 805-6890

Fig. 6a

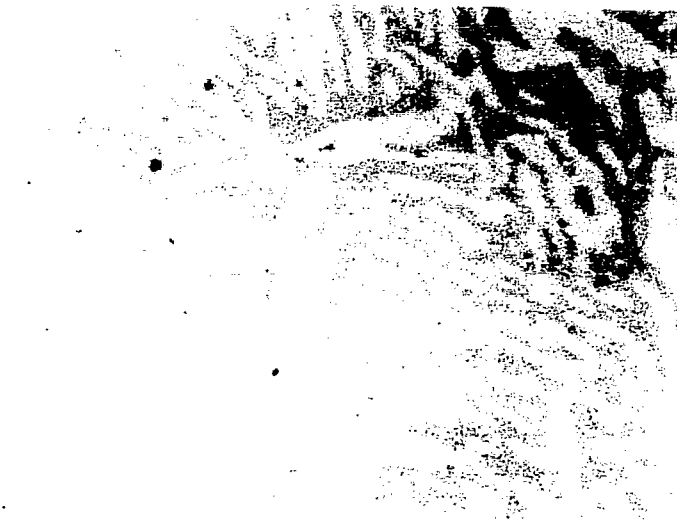

Fig. 6b

XBB 805-6391

Fig. 7a

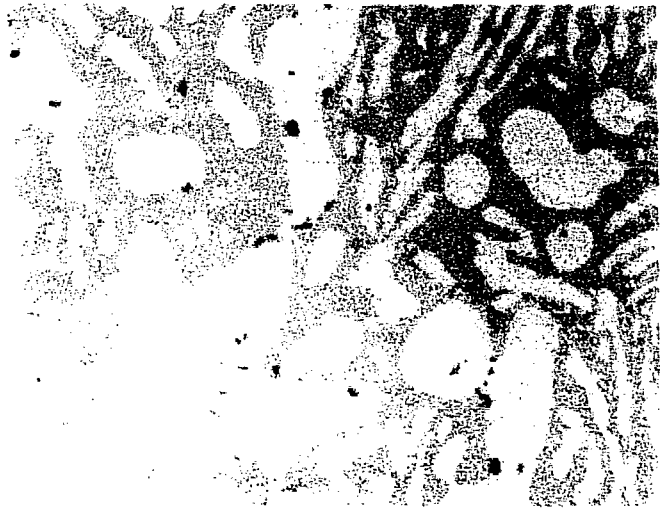

Fig. 7b

XBB 805-6892

Fig. 8a

Fig. 8b

XBB 805-6895

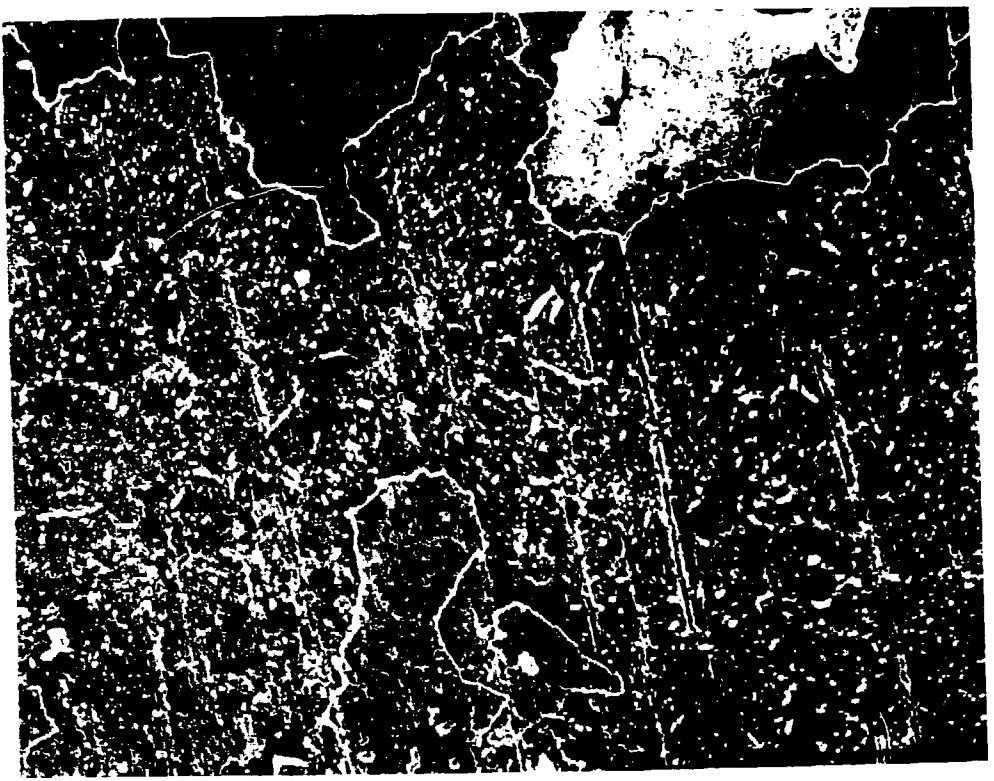

Fig. 9a

XBB 305-6866

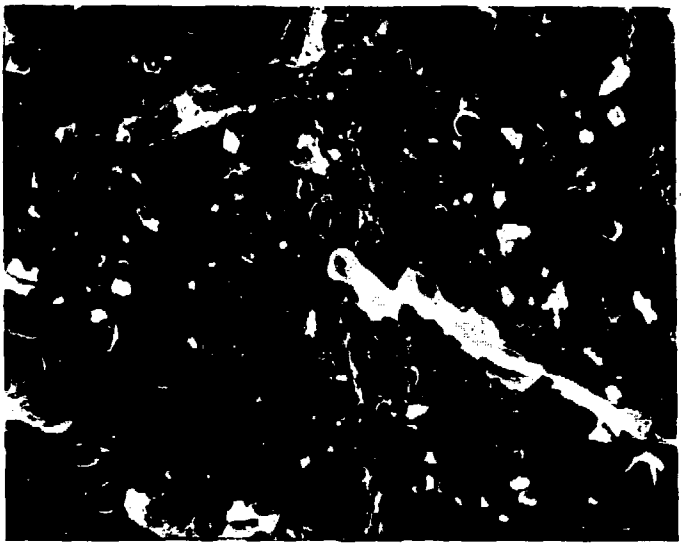

Fig. 9b

Fig. 9c XBB 305-6894

Fig. 10 XBB 805-6865

Fig. 11a

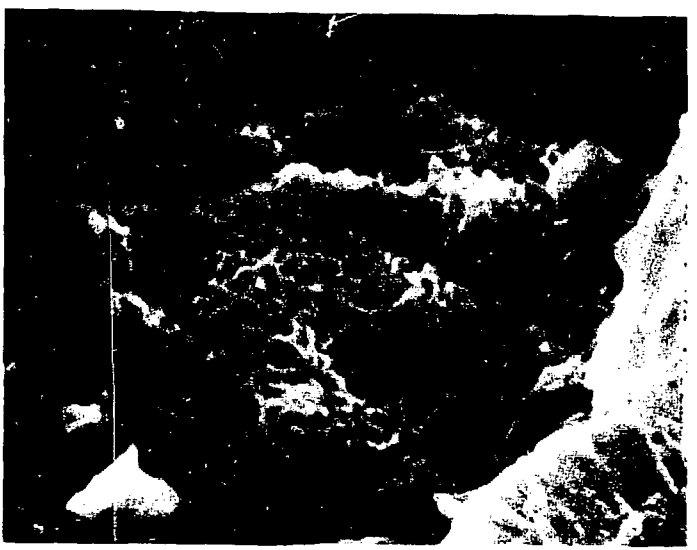

Fig. 11b XBB 805-6895

Fig. 12

XBB 805-6864

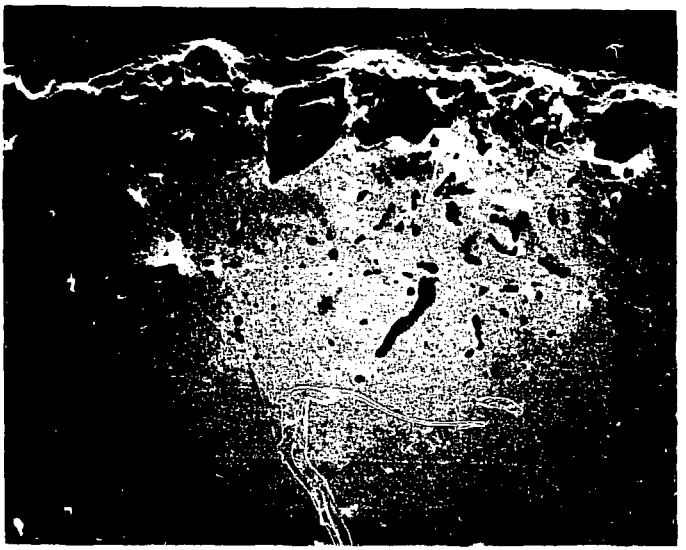

Fig. 13a

Fig. 13b XBB 805-6896

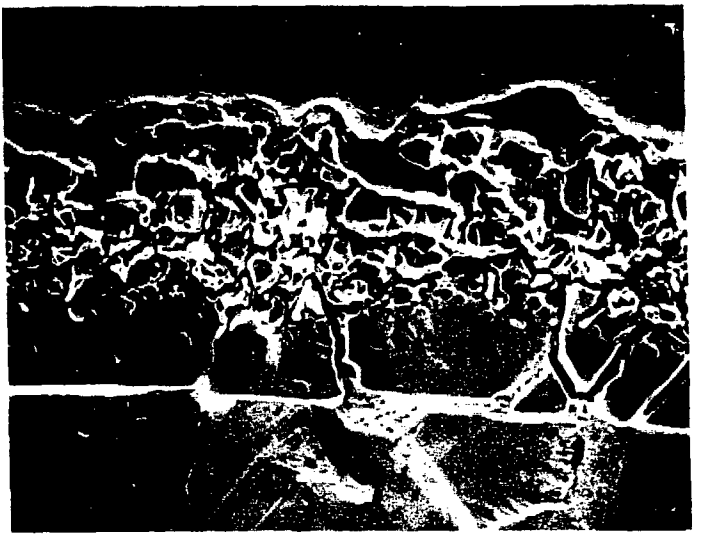

Fig. 15c

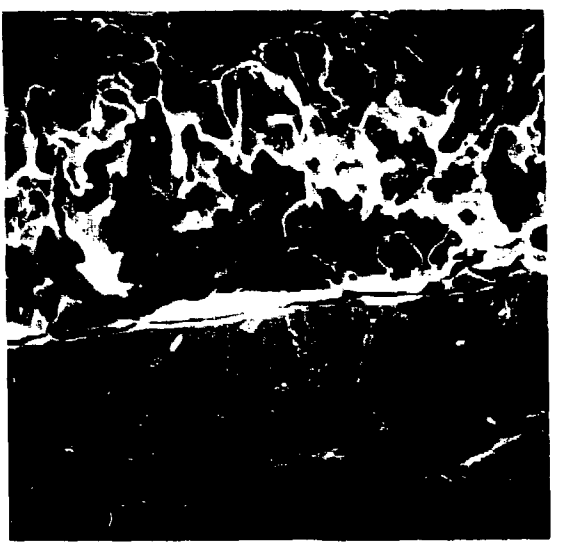

Fig. 15d

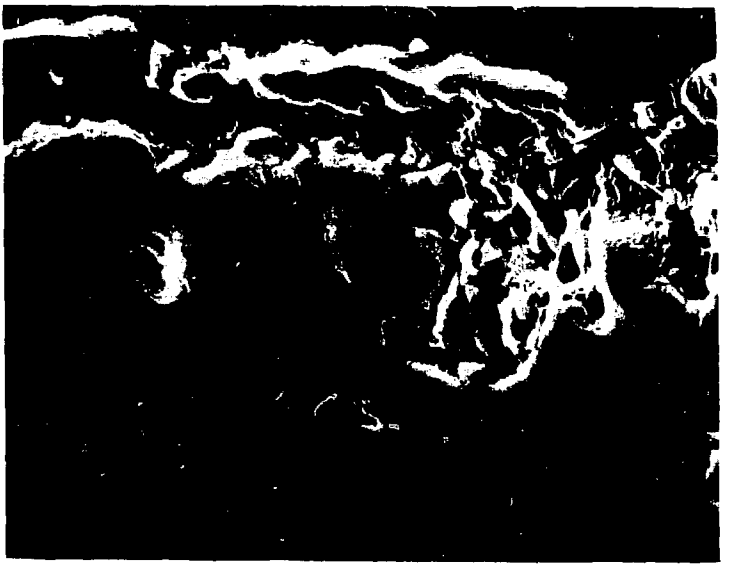

Fig. 14a

Fig. 14b XBB 805-6898

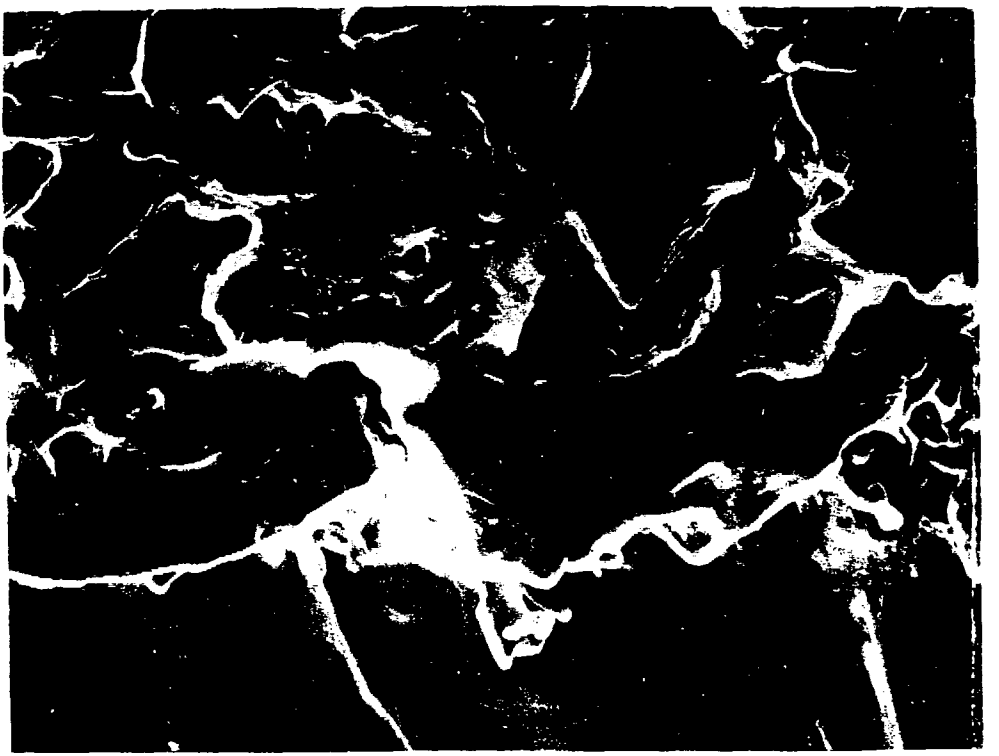

Fig. 14c XBB 805-6865

Fig. 15 XBB 805-6862

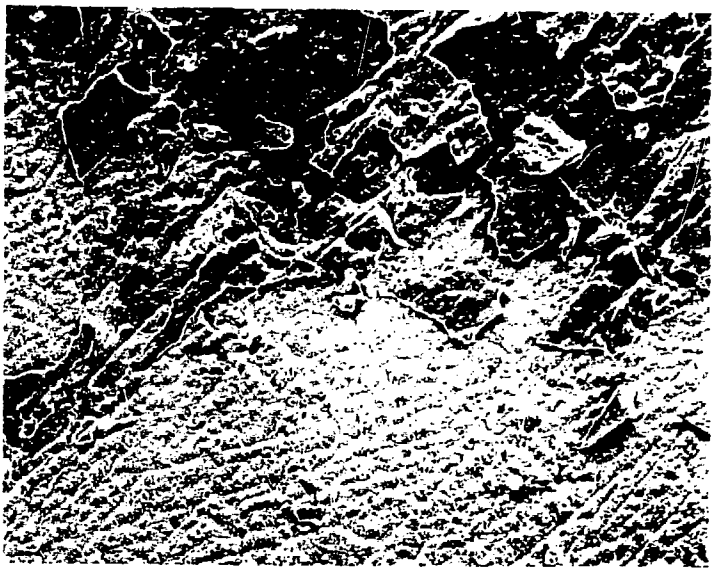

Fig. 16a

Fig. 16b

Fig. 16c

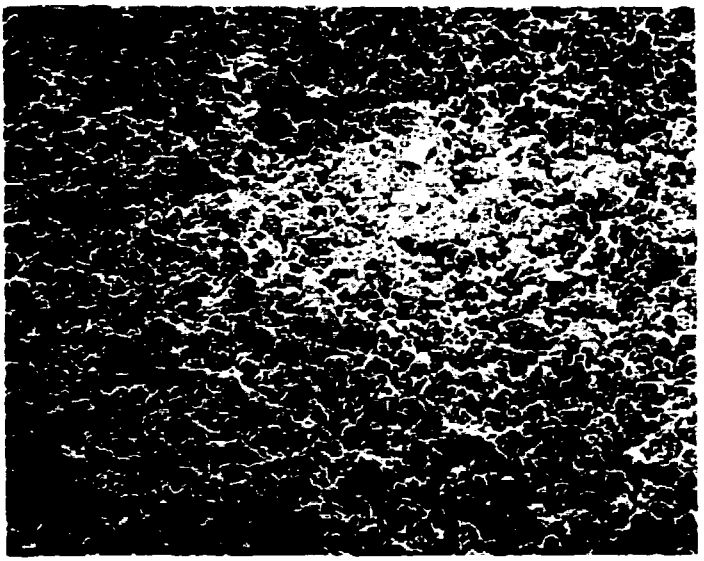

Fig. 17a

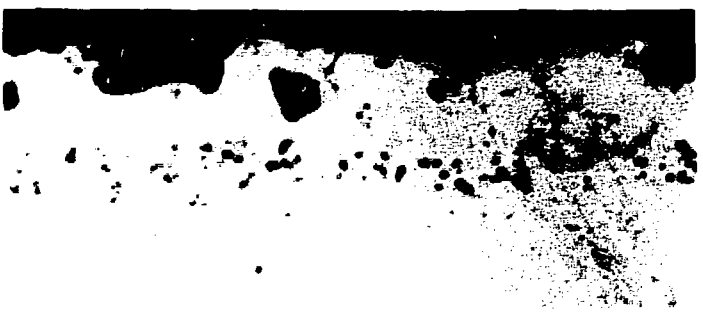

Fig. 17b XBB 805-6899

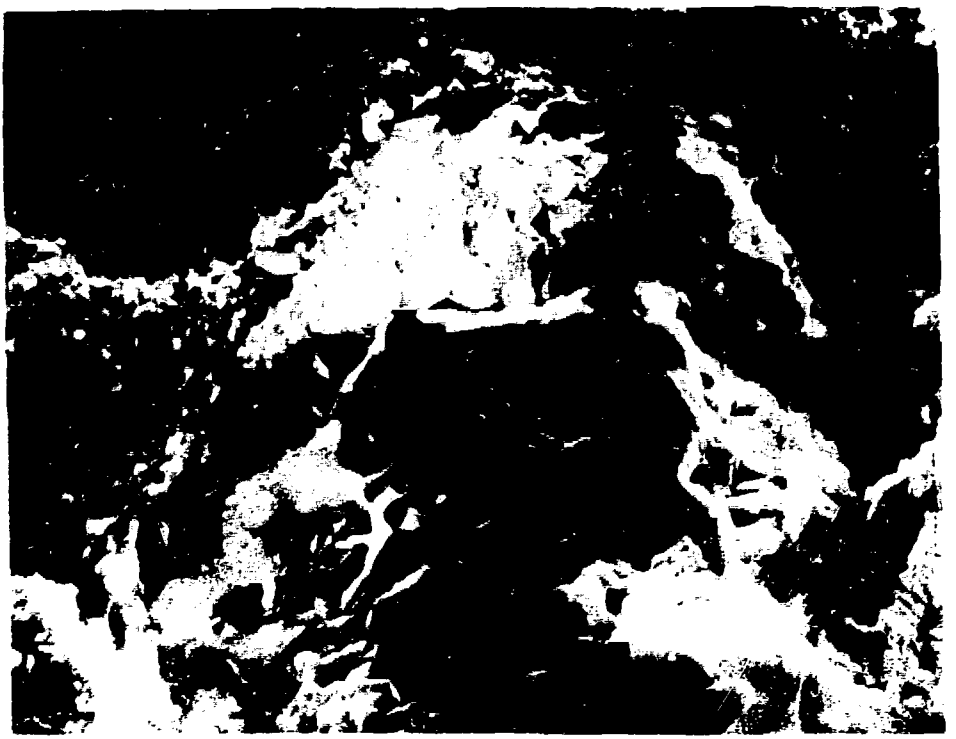

Fig. 17c XBB 805-6870

Fig. 18a

Fig. 18b XBB 805-6886

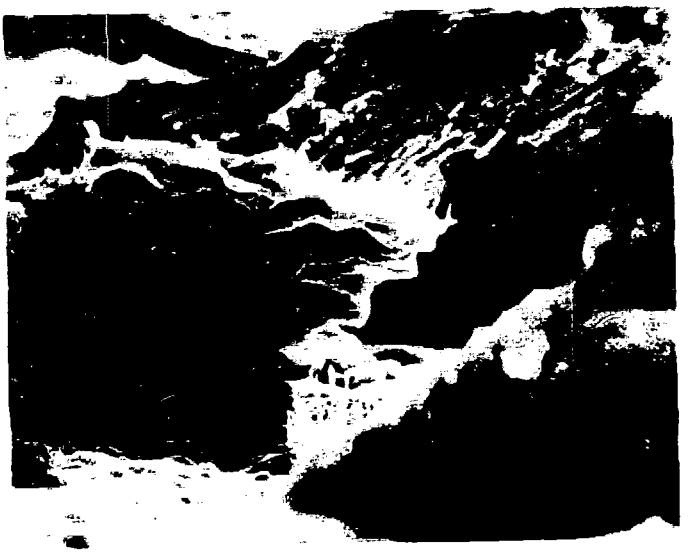

Fig. 18c

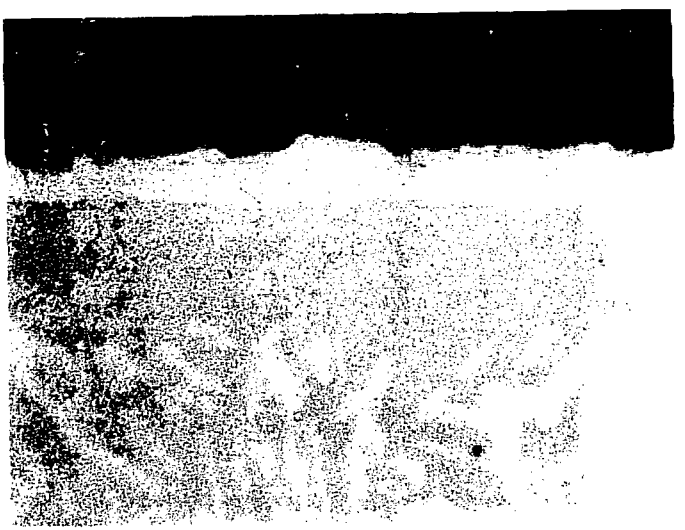

Fig. 18d XBB 805-6887

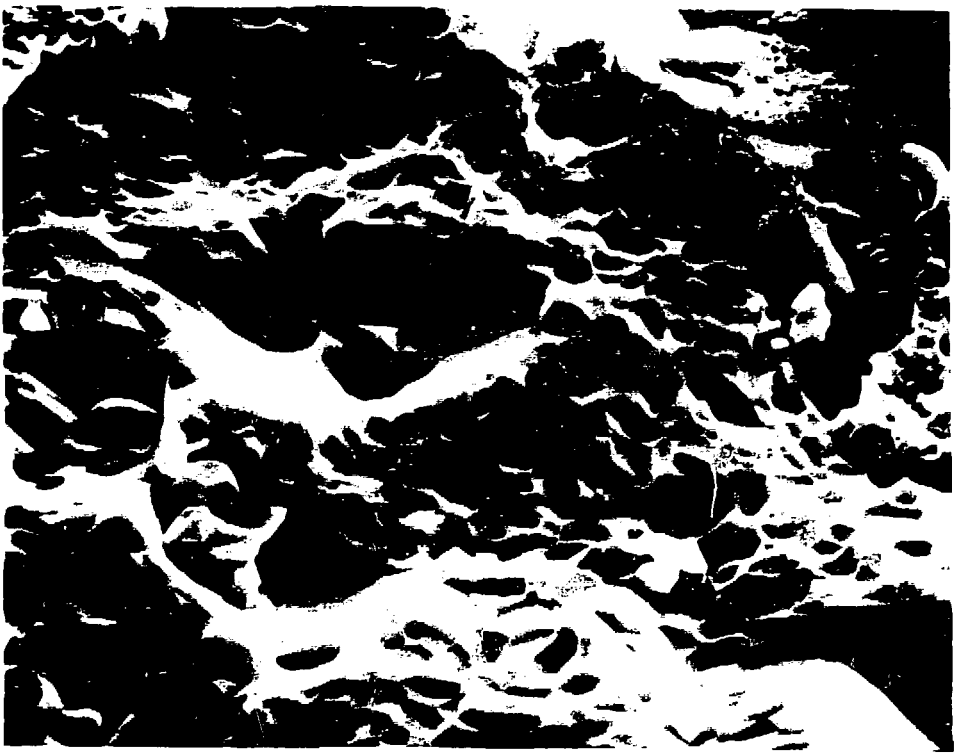

Fig. 18c XBB 805-6869

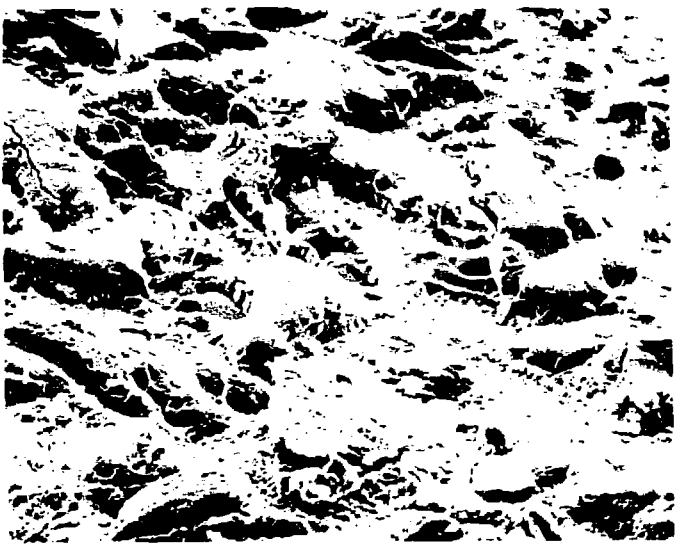

Fig. 19a

Fig. 19b XBB 805-6388

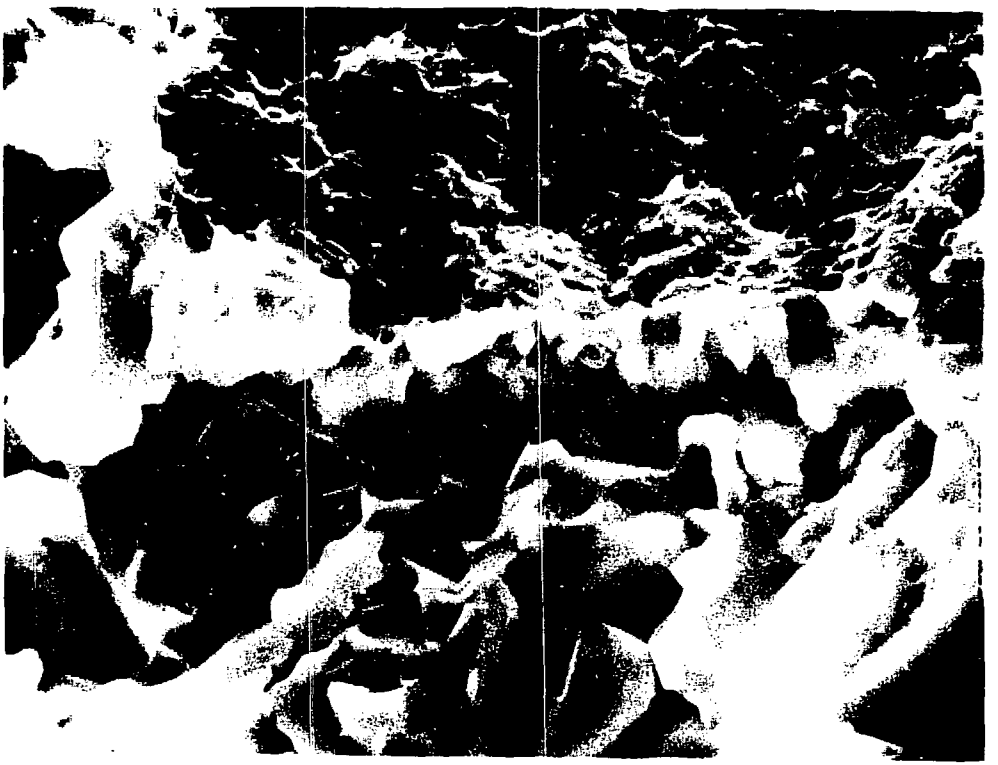

Fig. 19c XBB 805-6868

Fig. 20 XBB 805-6867

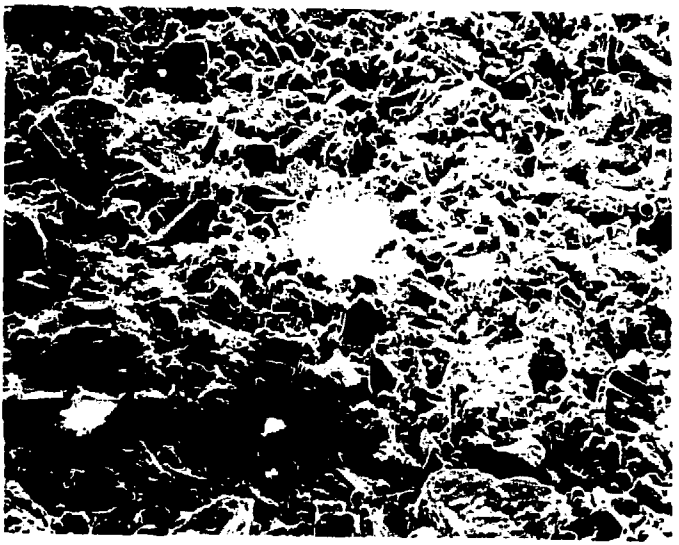

Fig. 21a

Fig. 21b XBB 805-6882

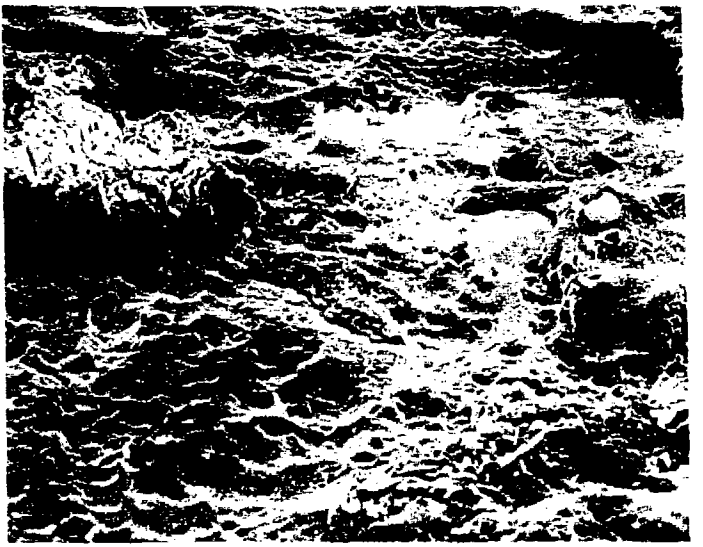

Fig. 22a

Fig. 22b XBB 805-6885

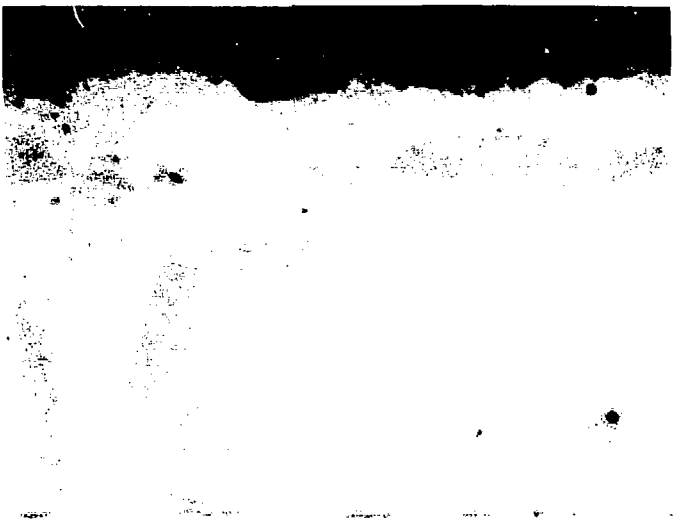

Fig. 22c

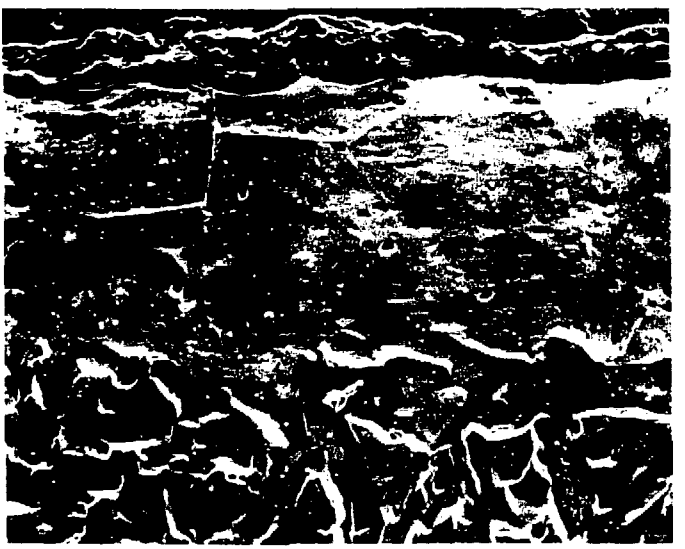

Fig. 22d XBB 305-6884

Fig. 22e XBB 805-6871

Fig. 23a

Fig. 23b XBB 805-6885

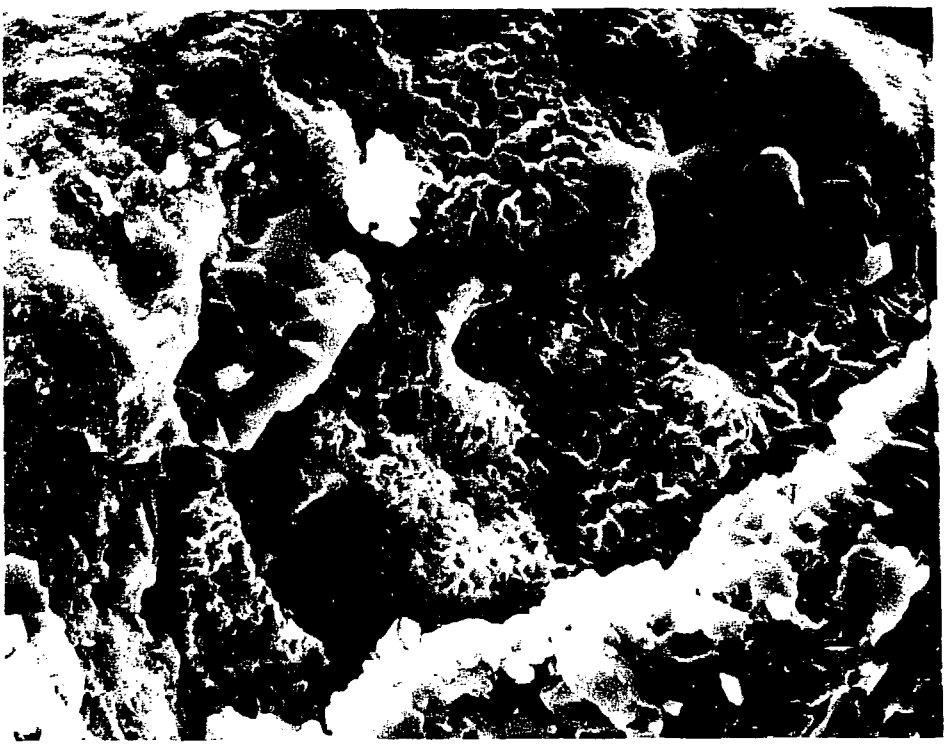

Fig. 23c XBB 805-6874

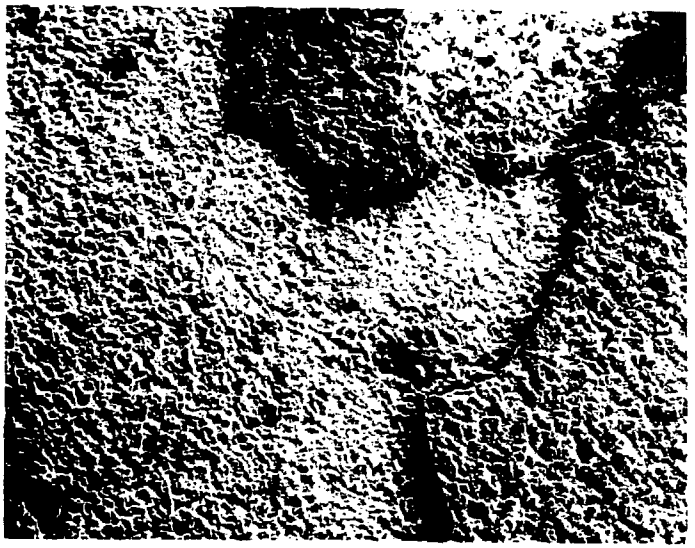

Fig. 24a

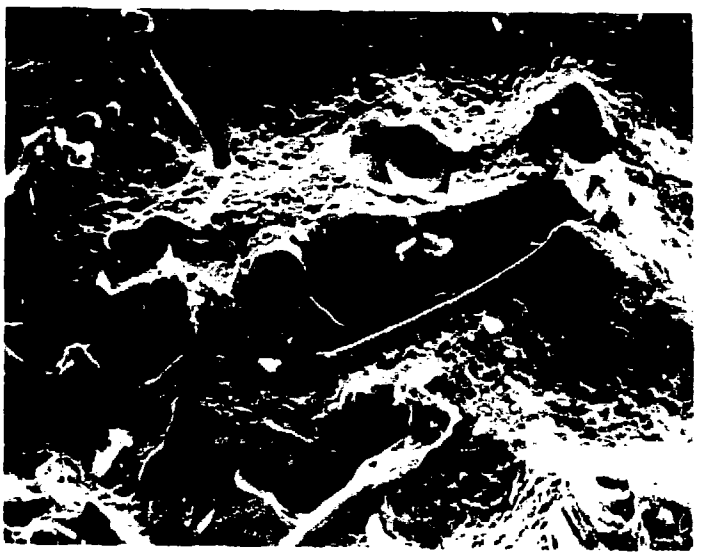

Fig. 24b XBB 805-6875

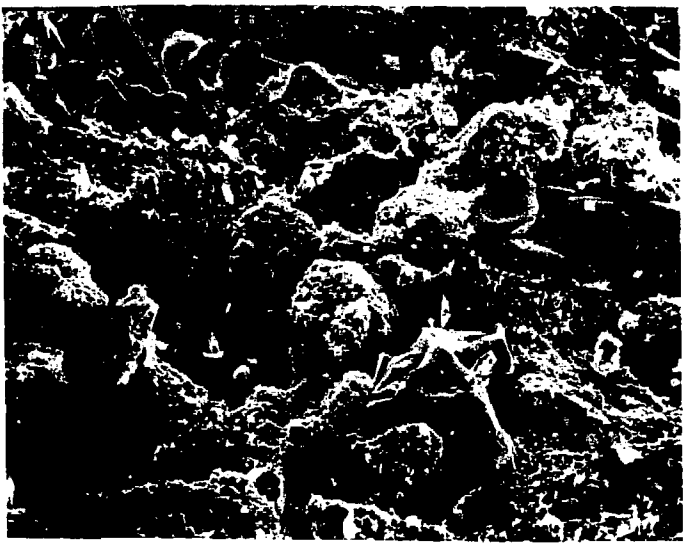

Fig. 25a

Fig. 25b XBB 805-6876

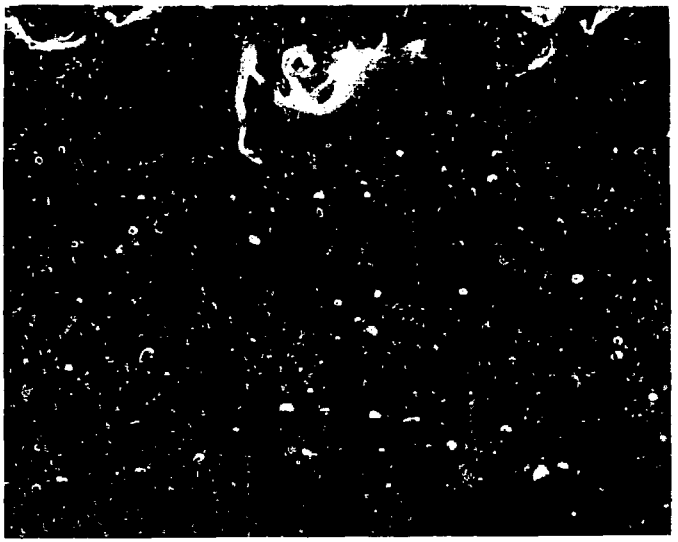

Fig. 25c

Fig. 25d

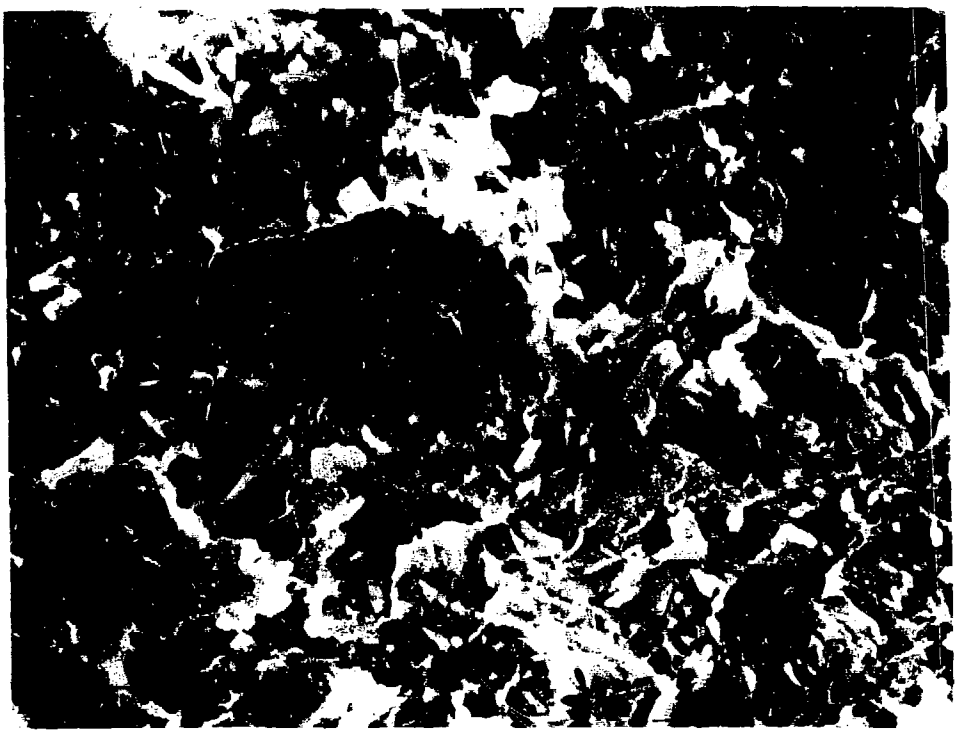

Fig. 25c XBB 805-6873

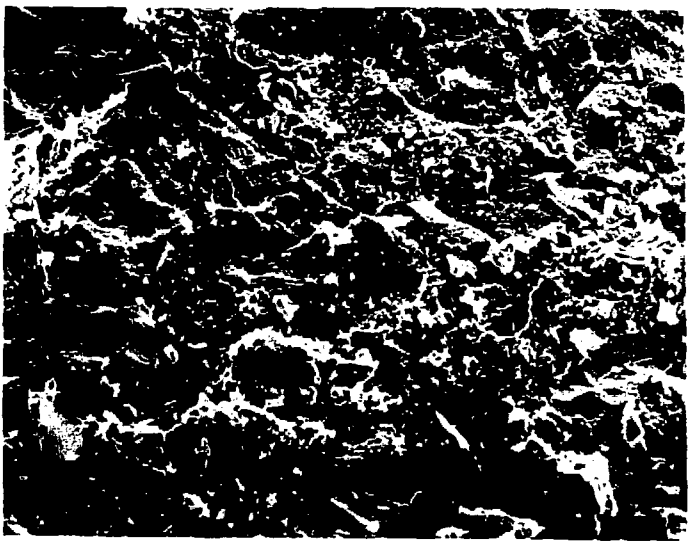

Fig. 26a

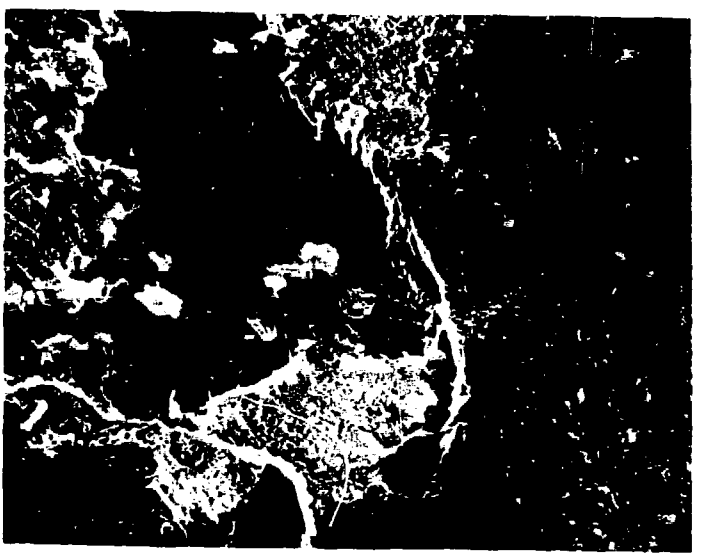

Fig. 26b XBB 805-6878

Fig. 26c

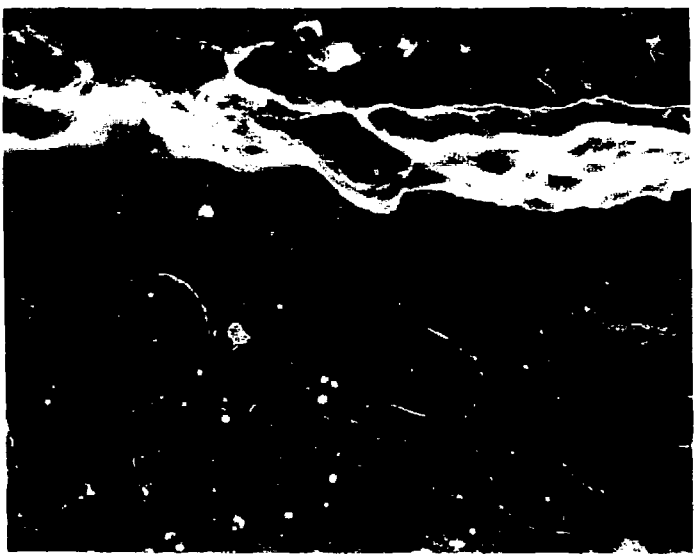

Fig. 26d XBB 805-6579

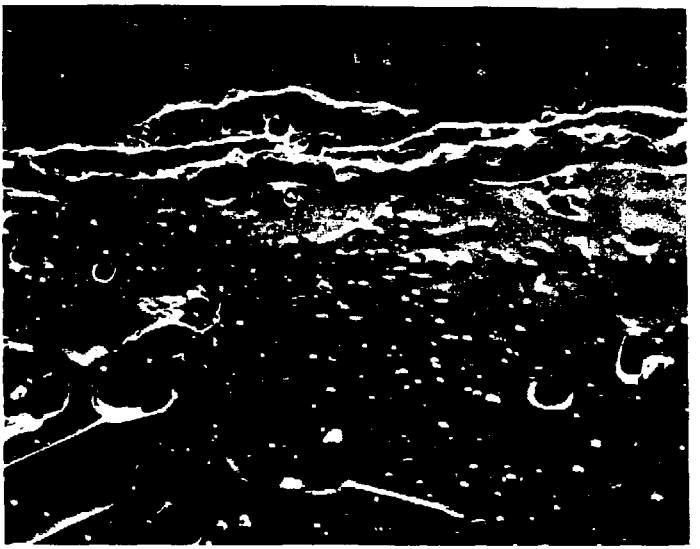

Fig. 26e

Fig. 26f XBB 805-6880

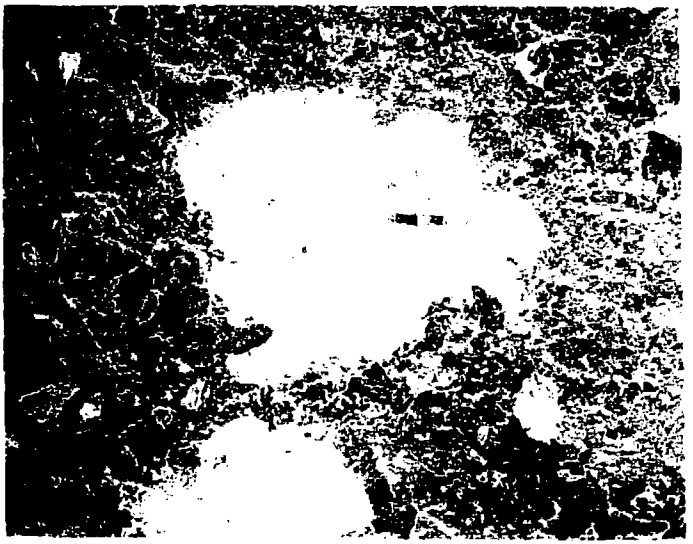

Fig. 27a

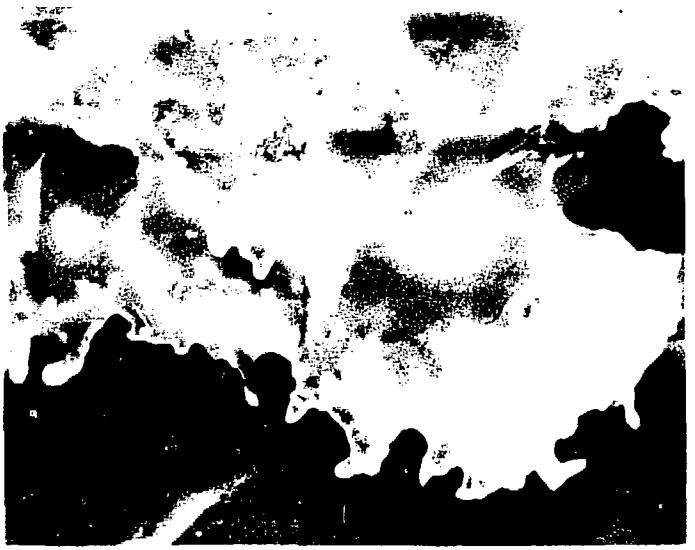

Fig. 27b XBB 305-6881

Fig. 27c XBB 805-6872

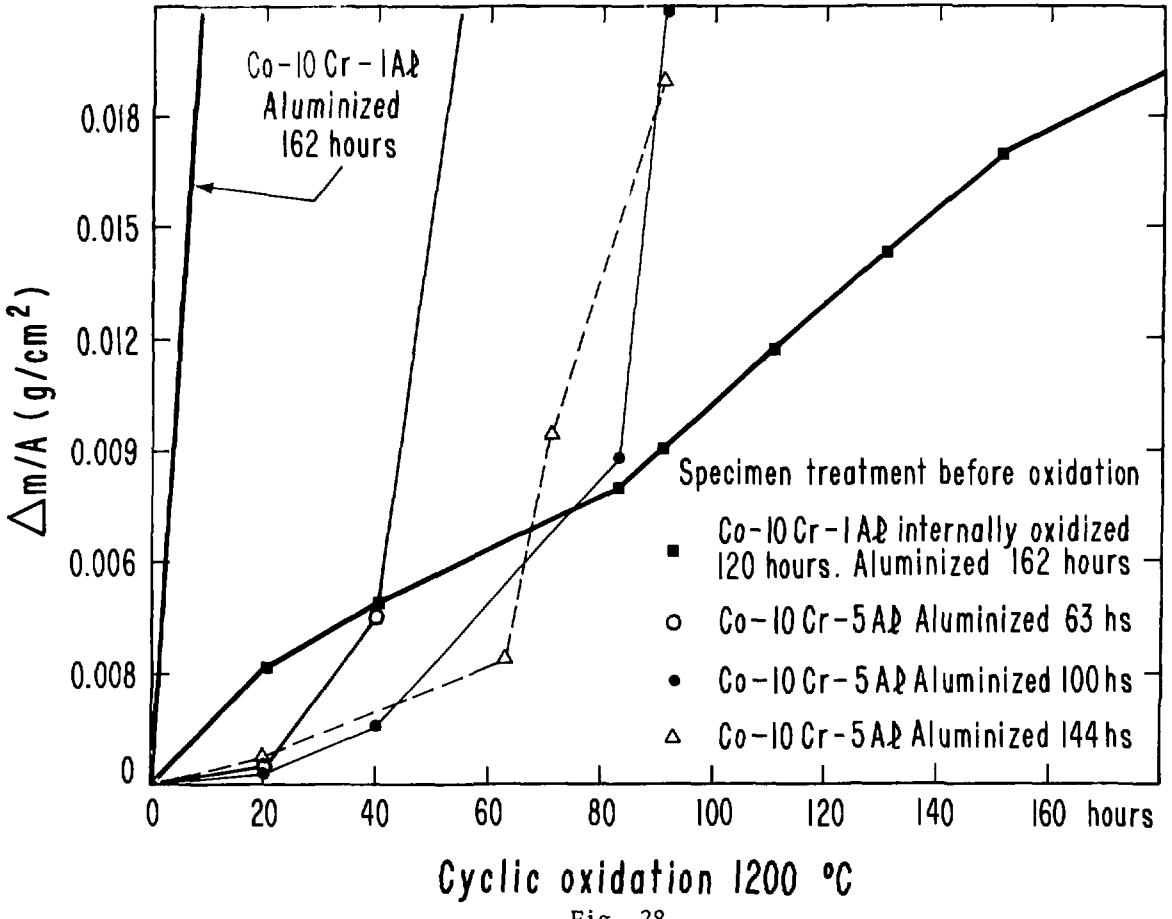

Fig. 28

XBL805-1087

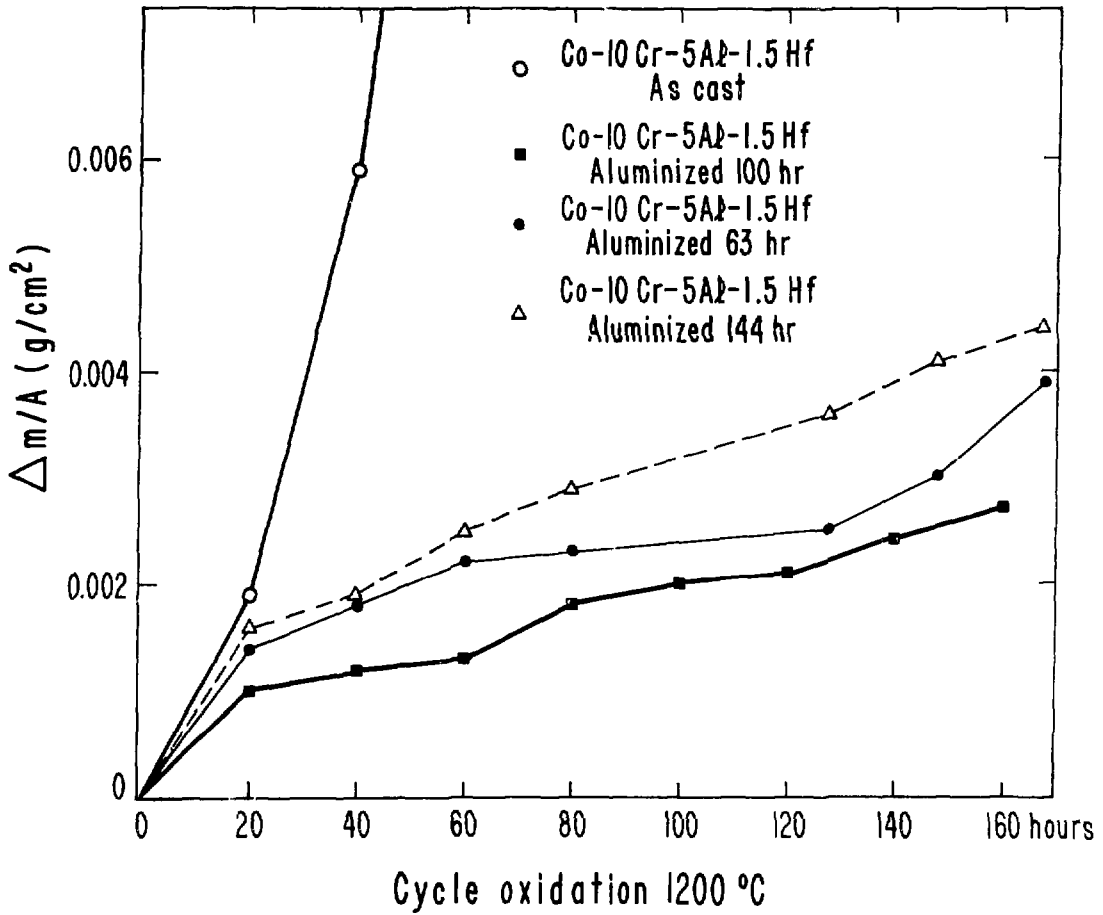

Fig. 29

XBL 805-1085

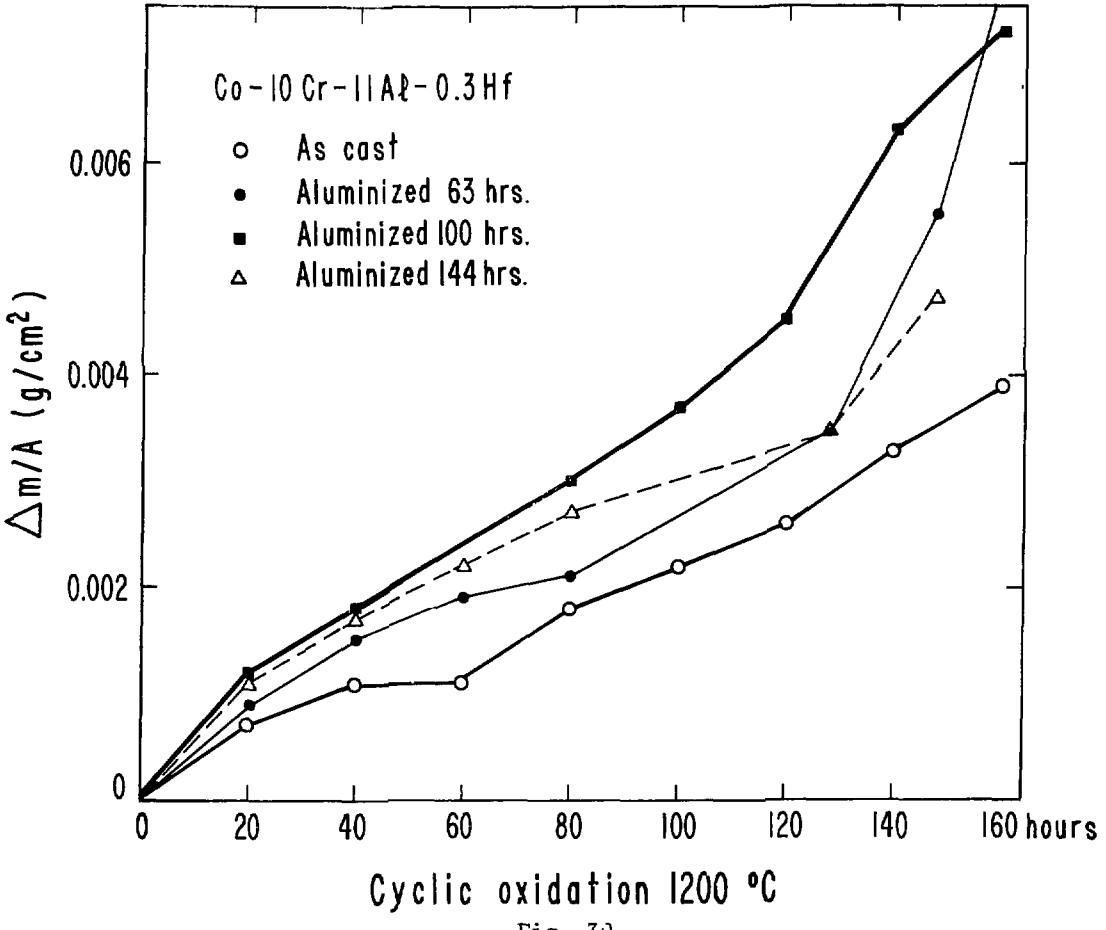

Fig. 30

XBL 805-1088

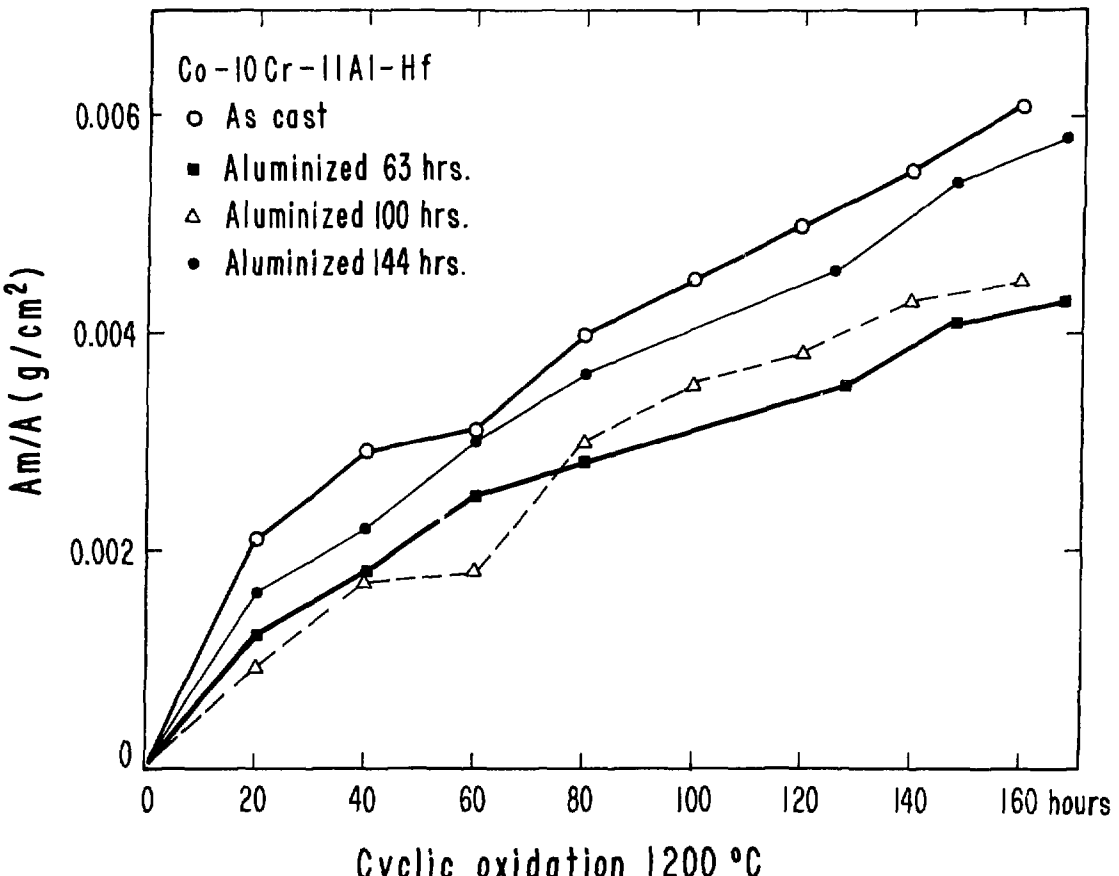

Fig. 31

XBL805-1090

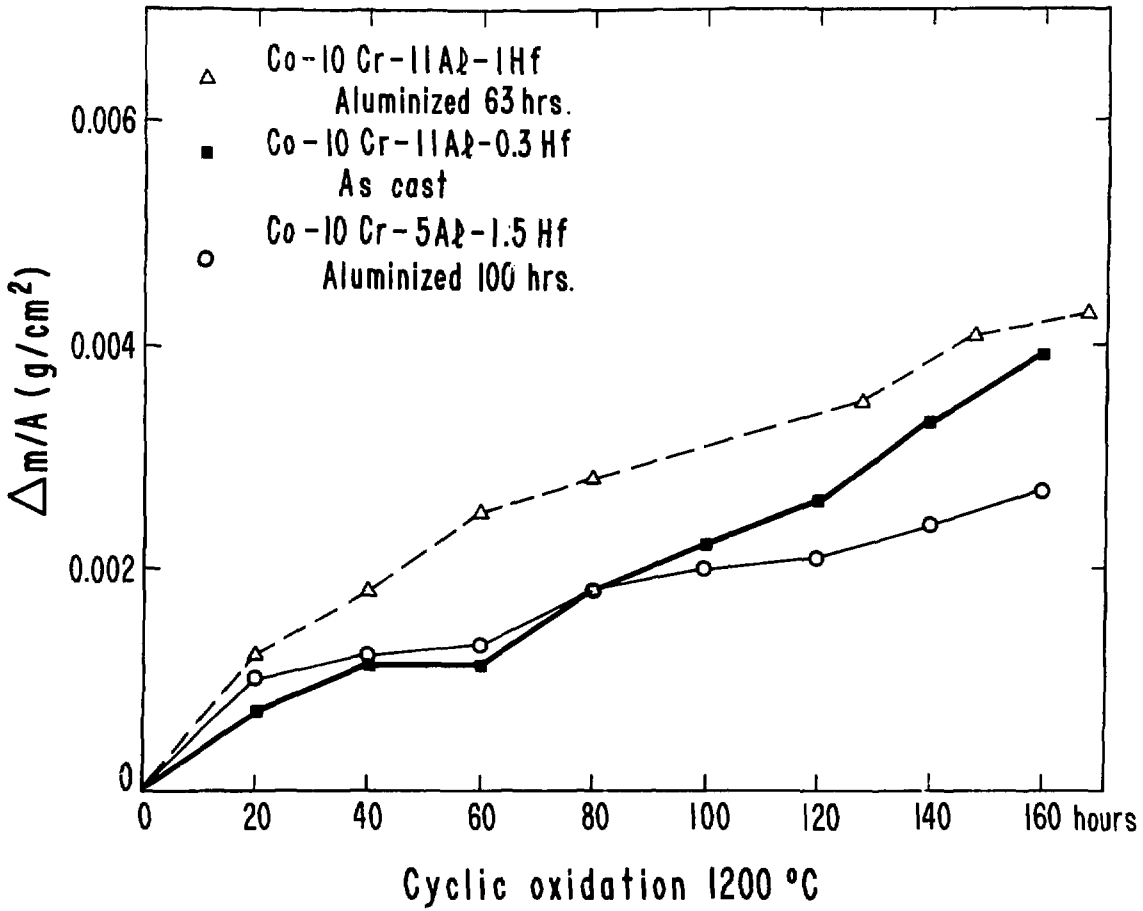

Fig. 32

XBL805-1089